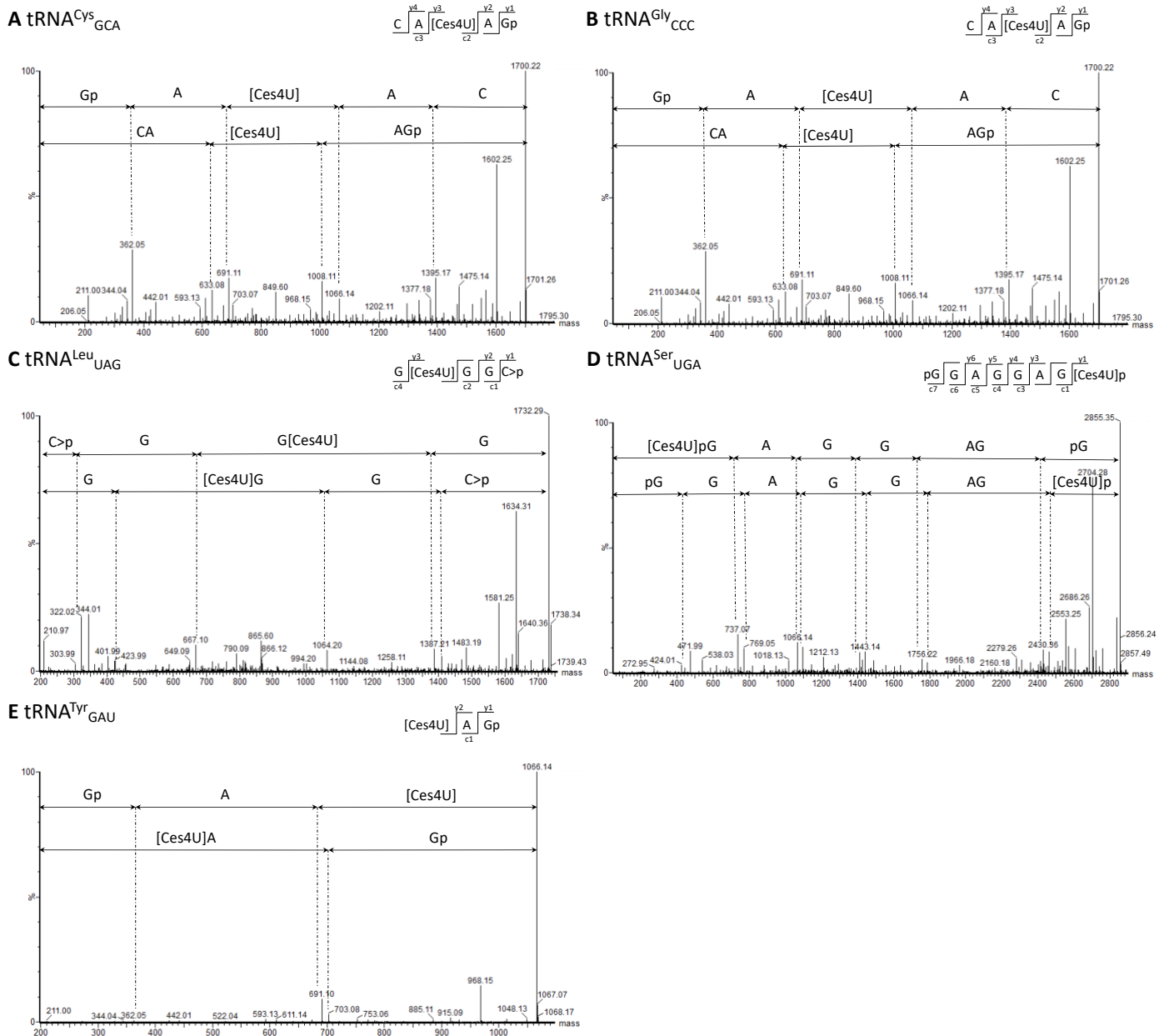
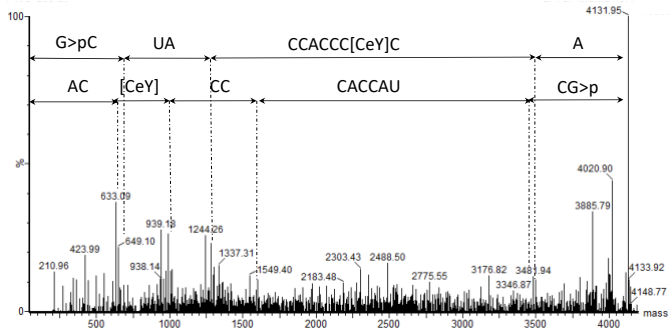
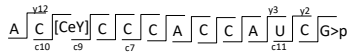
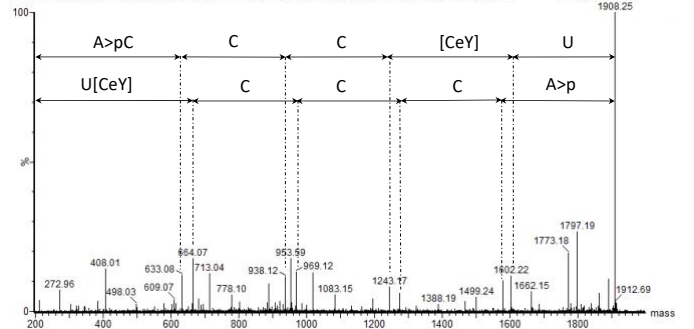
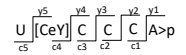
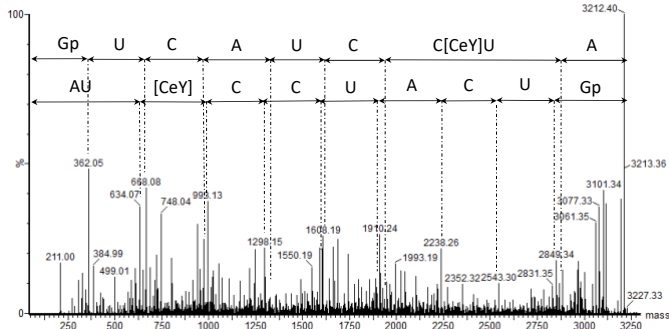
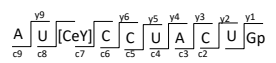
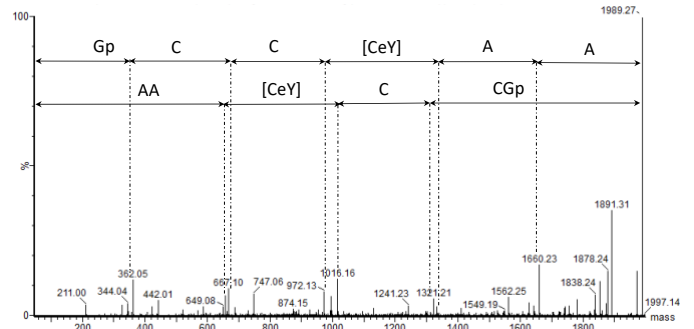
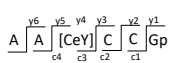
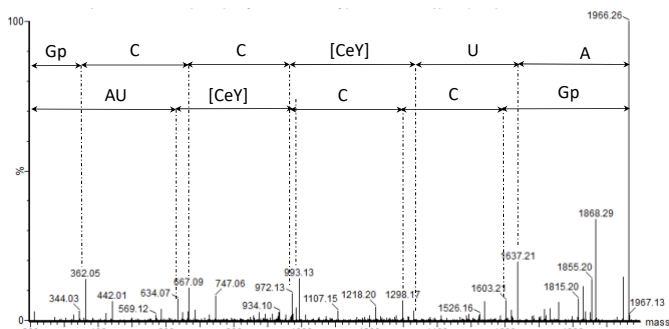
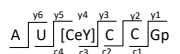
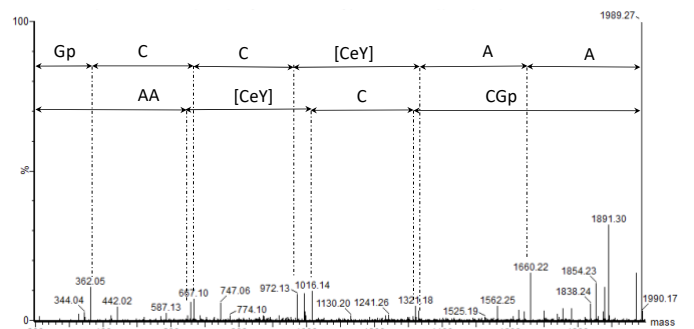
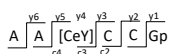
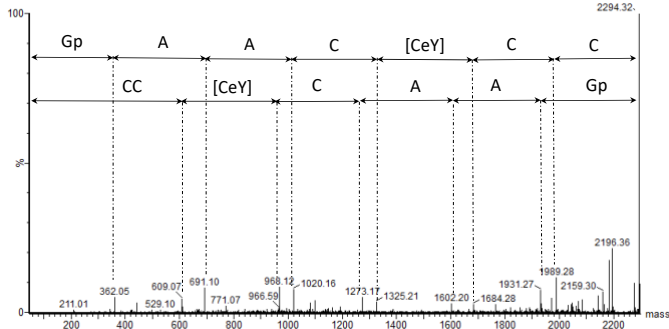
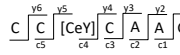
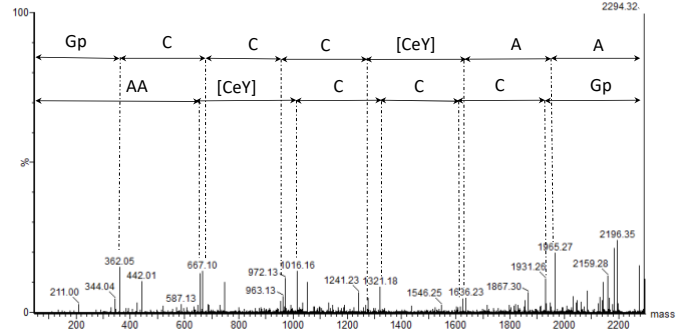
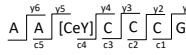
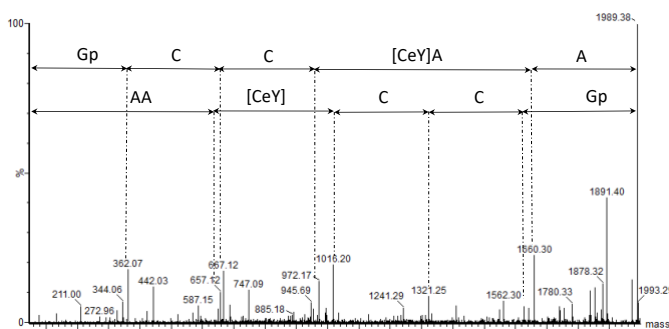
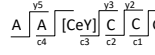


SUPPLEMENTARY MATERIAL

Temperature-dependent tRNA Modifications in Bacillales

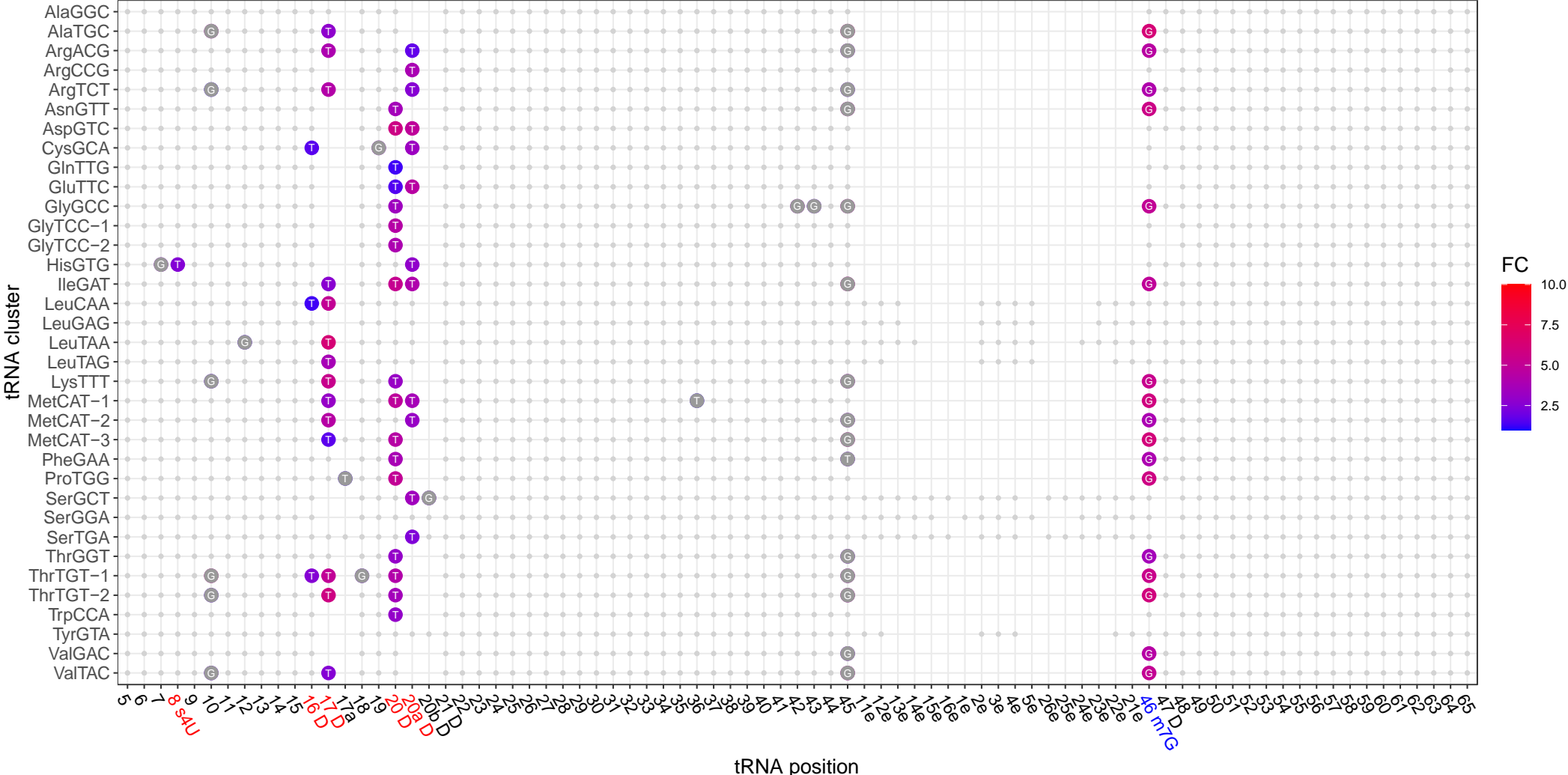


Suppl. Figure 1. Additional MS/MS sequencing spectra containing cyanoethylated 4-thiouridine (Ces⁴U) at tRNA position U8 of *G. stearothermophilus*. A) MS/MS spectrum CA[Ces⁴U]AGp of tRNA^{Cys}_{GCA} after RNase T₁ digestion (*m/z* 849.61 *z* = 2-). B) MS/MS spectrum UG[Ces⁴U]A>p of tRNA^{Gly}_{CCC} after RNase U₂ digestion (*m/z* 676,56 *z* = 2-). C) MS/MS spectrum G[Ces⁴U]GGC>p of tRNA^{Leu}_{UAG} after RNase A digestion (*m/z* 865.63 *z* = 2-). D) MS/MS spectrum pGGAGGAG[Ces⁴U]p of tRNA^{Ser}_{UGA} after RNase A digestion (*m/z* 1427.18 *z* = 2-). E) MS/MS spectrum [Ces⁴U]AGp of tRNA^{Tyr}_{GAU} after RNase T₁ digestion (*m/z* 1066.13 *z* = 1-).

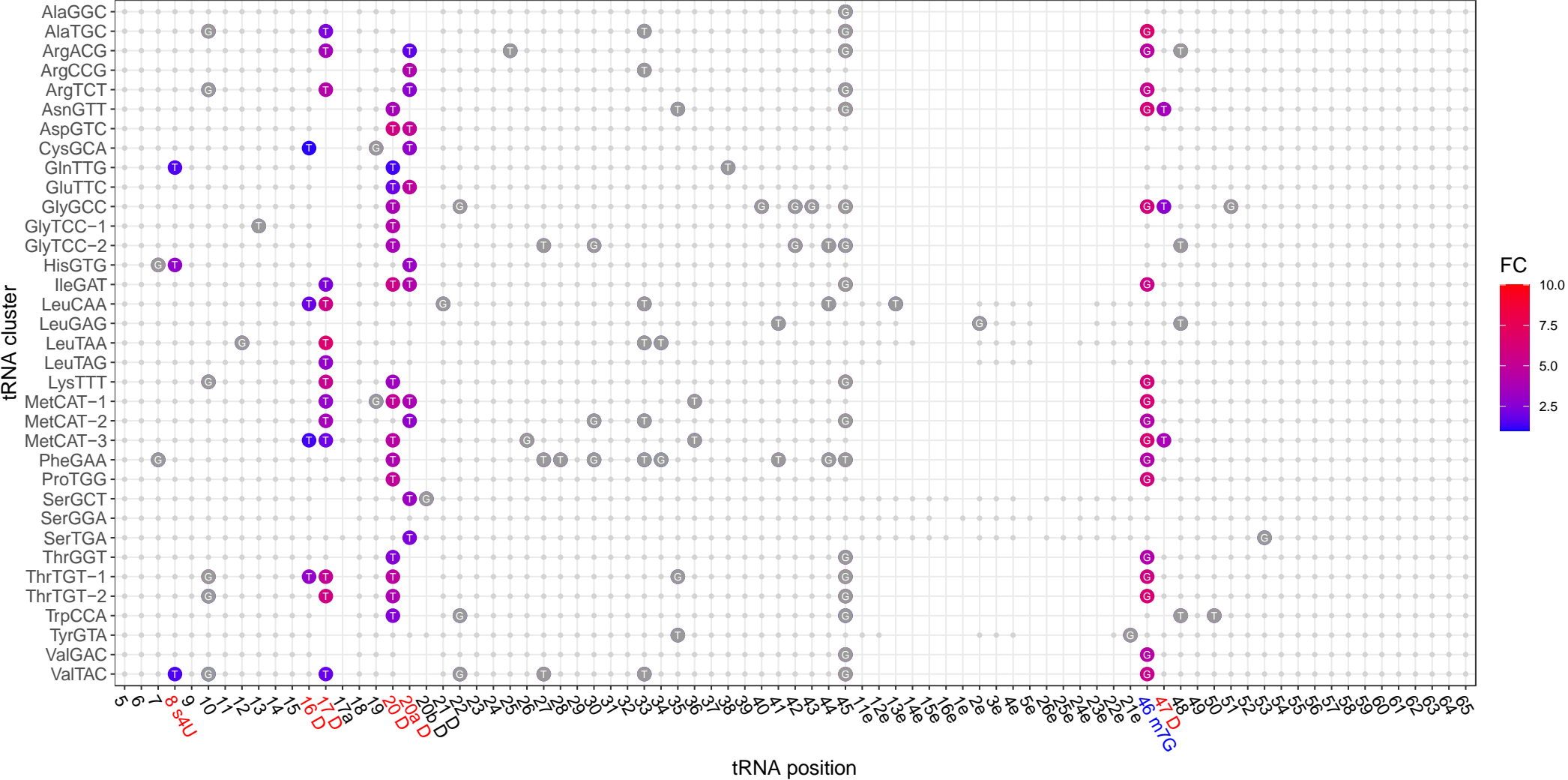
A tRNA^{Leu}_{CAA}**B** tRNA^{His}_{GUG}**C** tRNA^{Trp}_{CCA}**D** tRNA^{Tyr}_{GAU}**E** tRNA^{Phe}_{GAA}**F** tRNA^{Cys}_{GCA}**G** tRNA^{Ser}_{GGA}**H** tRNA^{Glu}_{UUC}**I** tRNA^{Ala}_{CGC}

Suppl. Figure 2. MS/MS sequencing spectra containing cyanoethylated pseudouridine (CeΨ) at tRNA position U60 of *G. stearothermophilus*. **A)** MS/MS spectrum AC[CeΨ]CCCACCAUCGp of tRNA^{Leu}_{CAA} after RNase T₁ digestion (m/z 1376.64 $z = 2$ -). **B)** MS/MS spectrum U[CeΨ]CCCA>p of tRNA^{His}_{GUG} after RNase U₂ digestion (m/z 953.62 $z = 2$ -). **C)** MS/MS spectrum AU[CeΨ]CCUACUGp of tRNA^{Trp}_{CCA} after RNase T₁ digestion (m/z 1070.13 $z = 2$ -). **D)** MS/MS spectrum AA[CeΨ]CCGp of tRNA^{Tyr}_{GAU} after RNase T₁ digestion (m/z 994.14 $z = 2$ -). **E)** MS/MS spectrum AU[CeΨ]CCGp of tRNA^{Phe}_{GAA} after RNase T₁ digestion (m/z 982.62 $z = 2$ -). **F)** MS/MS spectrum AA[CeΨ]CCGp of tRNA^{Cys}_{GCA} after RNase T₁ digestion (m/z 994.14 $z = 2$ -). **G)** MS/MS spectrum CC[CeΨ]CAAGp of tRNA^{Ser}_{GGA} after RNase T₁ digestion (m/z 1146.65 $z = 2$ -). **H)** MS/MS spectrum AA[CeΨ]CCCGp of tRNA^{Glu}_{UUC} after RNase T₁ digestion (m/z 1146.67 $z = 2$ -). **I)** MS/MS spectrum AA[CeΨ]CCGp of tRNA^{Ala}_{CGC} after RNase T₁ digestion (m/z 994.19 $z = 2$ -).

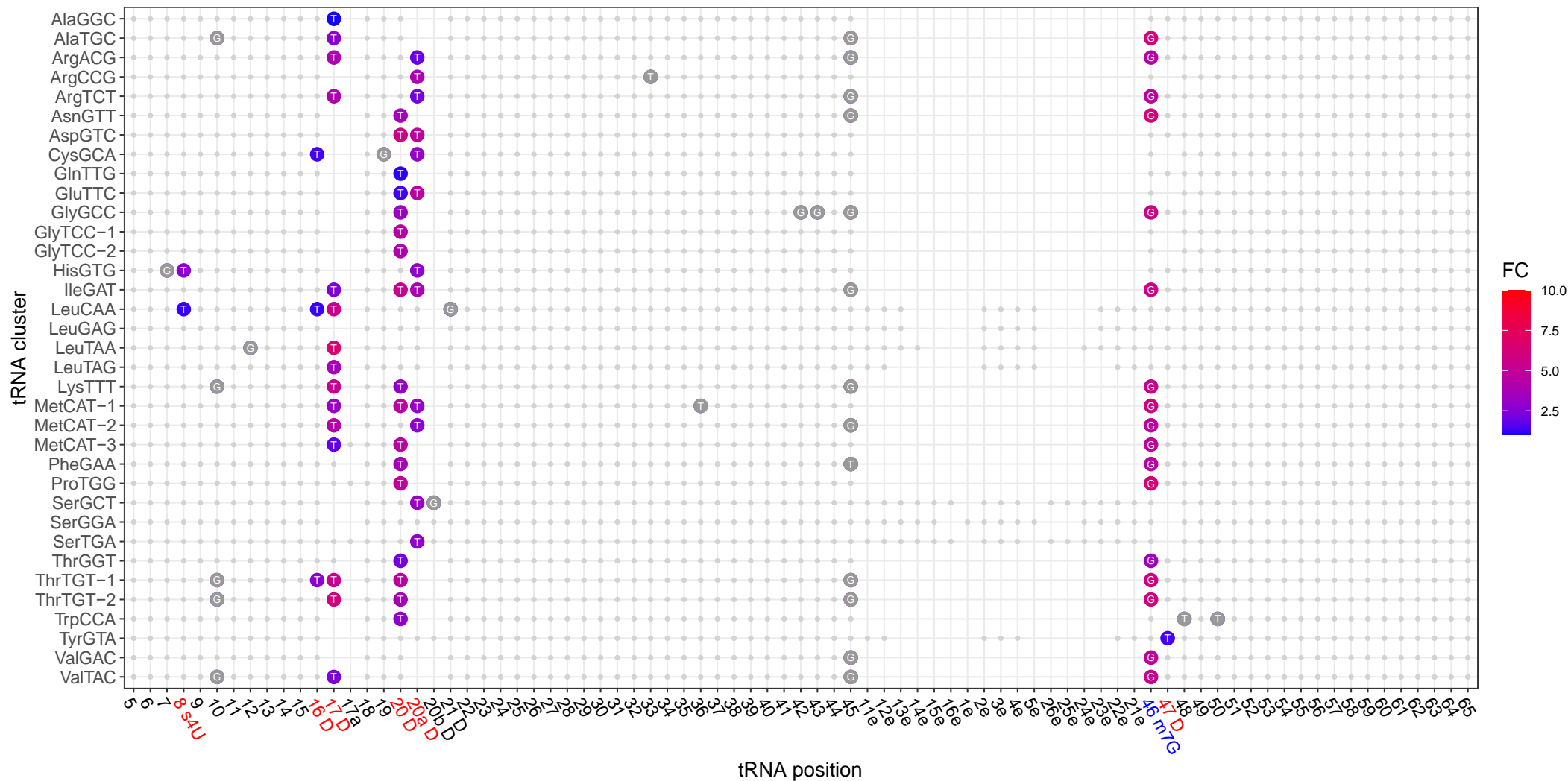
***P. halocryophilus*, 10°C**



P. halocryophilus, 20°C

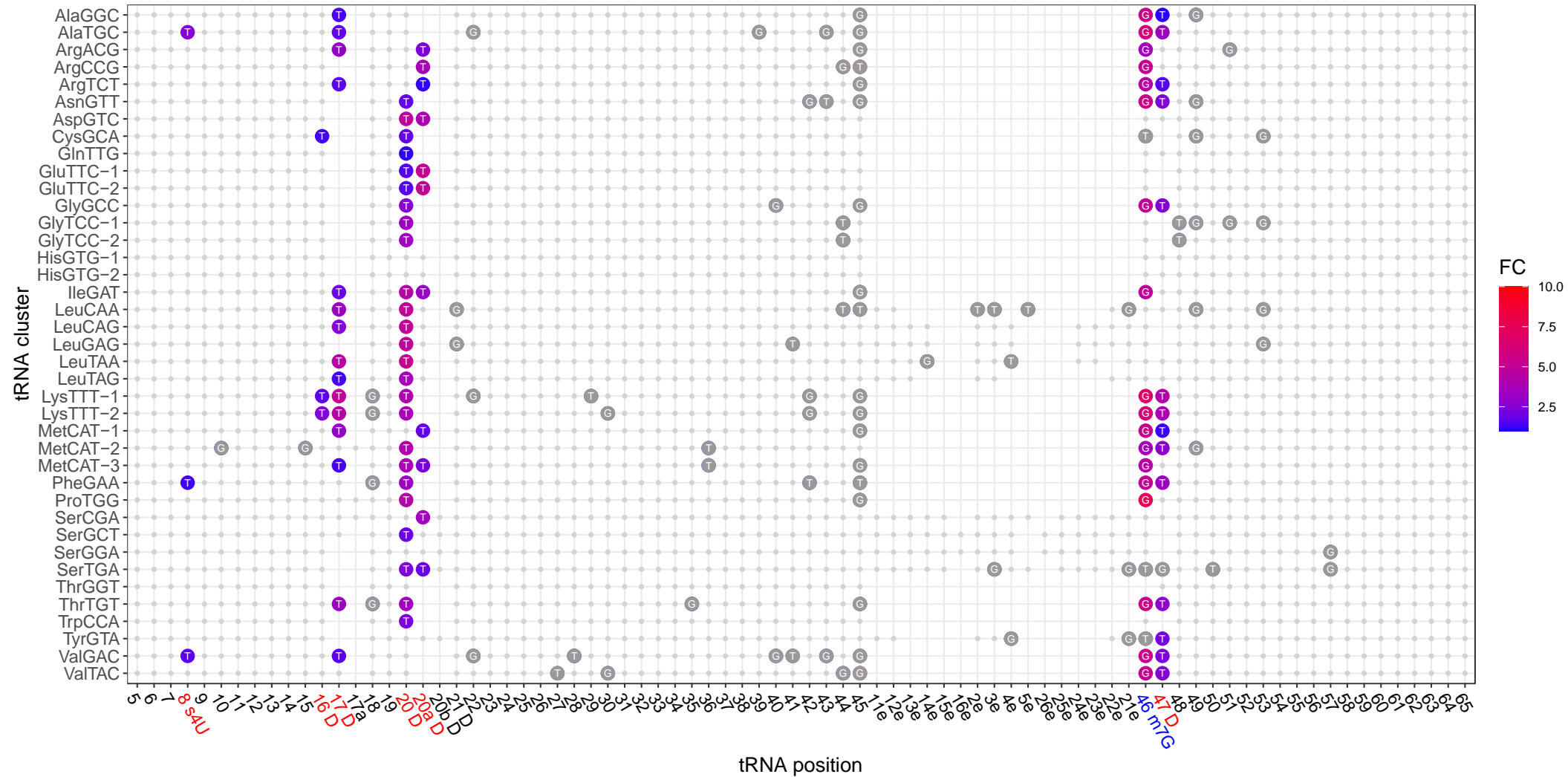


***P. halocryophilus*, 30°C**

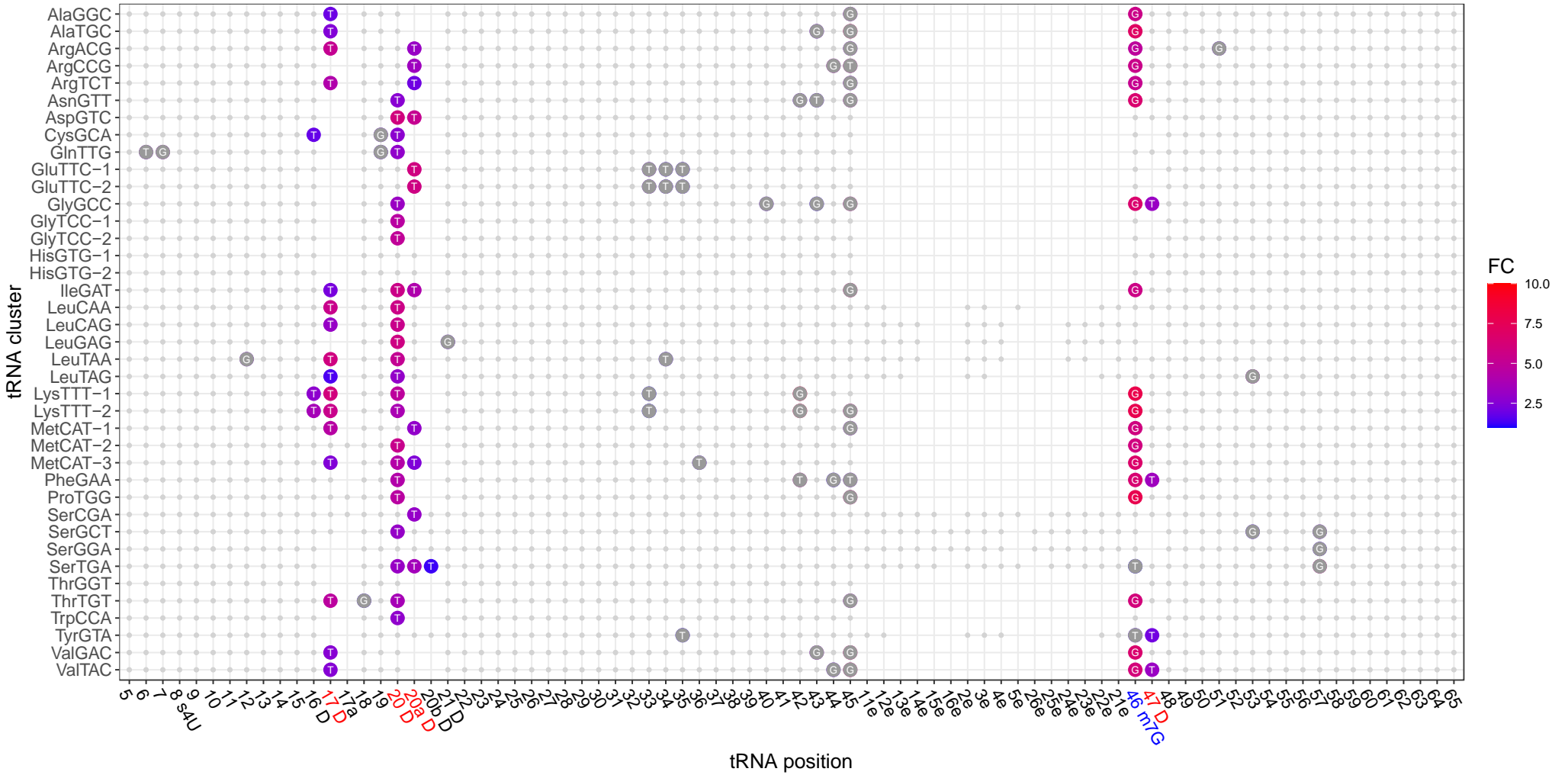


Suppl. Figure 3: Read termination sites from NaBH₄-treated RNA seq data of *P. halocryophilus*. The figure illustrates the investigated read termination (RT) sites for each tRNA cluster and tRNA position of *P. halocryophilus* at each growth temperature studied. All tRNA positions exhibiting a significant (adj. P value < 0.01) and strong (fold change (FC) ≥ 1, total number of RTs ≥ 20, and percentage of RTs ≥ 2) RT sites are color-coded from blue to red based on the logarithmic FC if the RT sites are classified as true positives. Type I false positive points are colored in gray. tRNA sites with no RT enrichment are represented as smaller gray dots. Enhanced RT sites were identified by comparing the RNA seq mapping profiles of sodium borohydride (NaBH₄)-treated samples with those of untreated control samples.

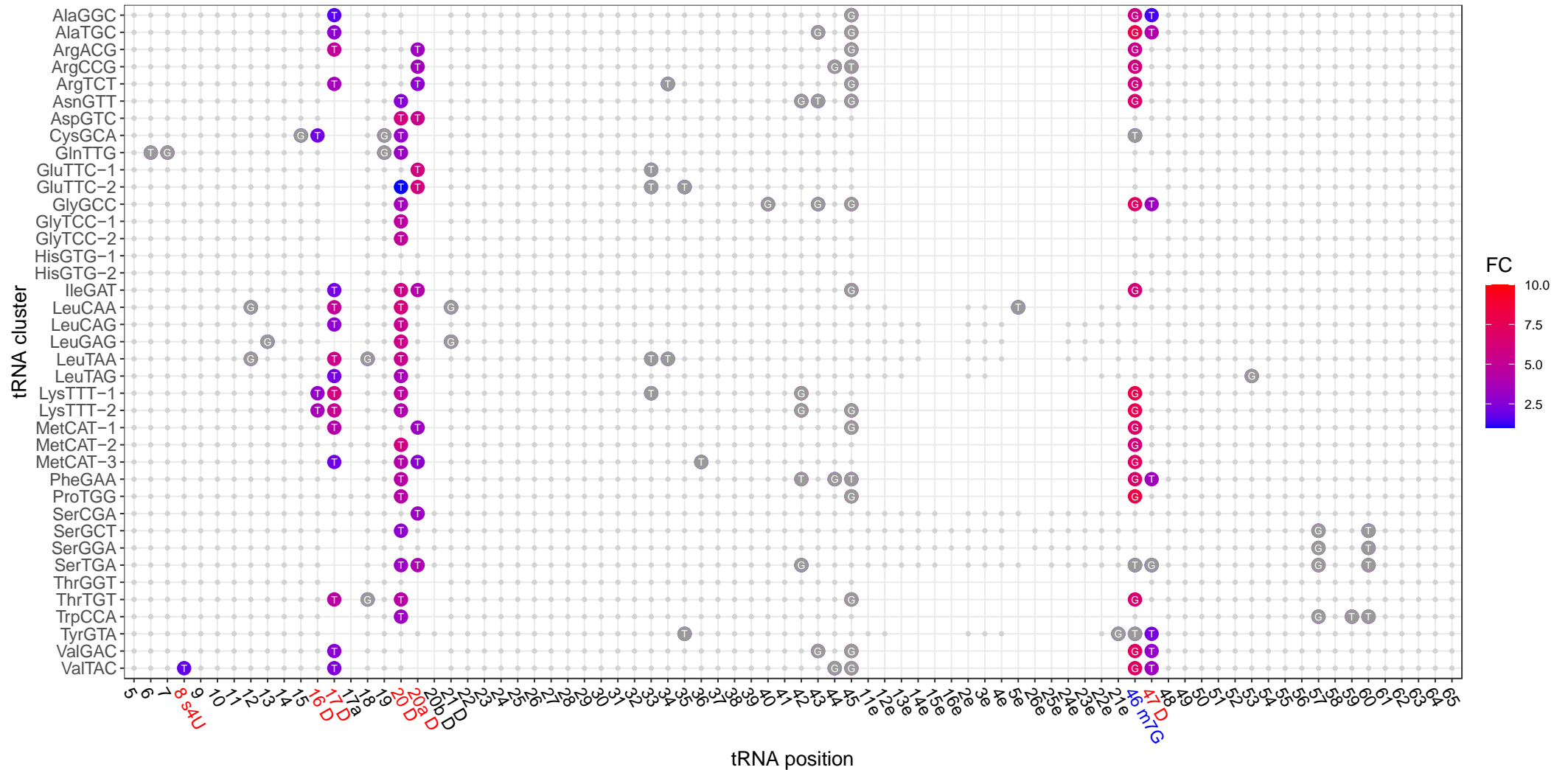
E. sibiricum, 10°C



***E. sibiricum*, 20°C**

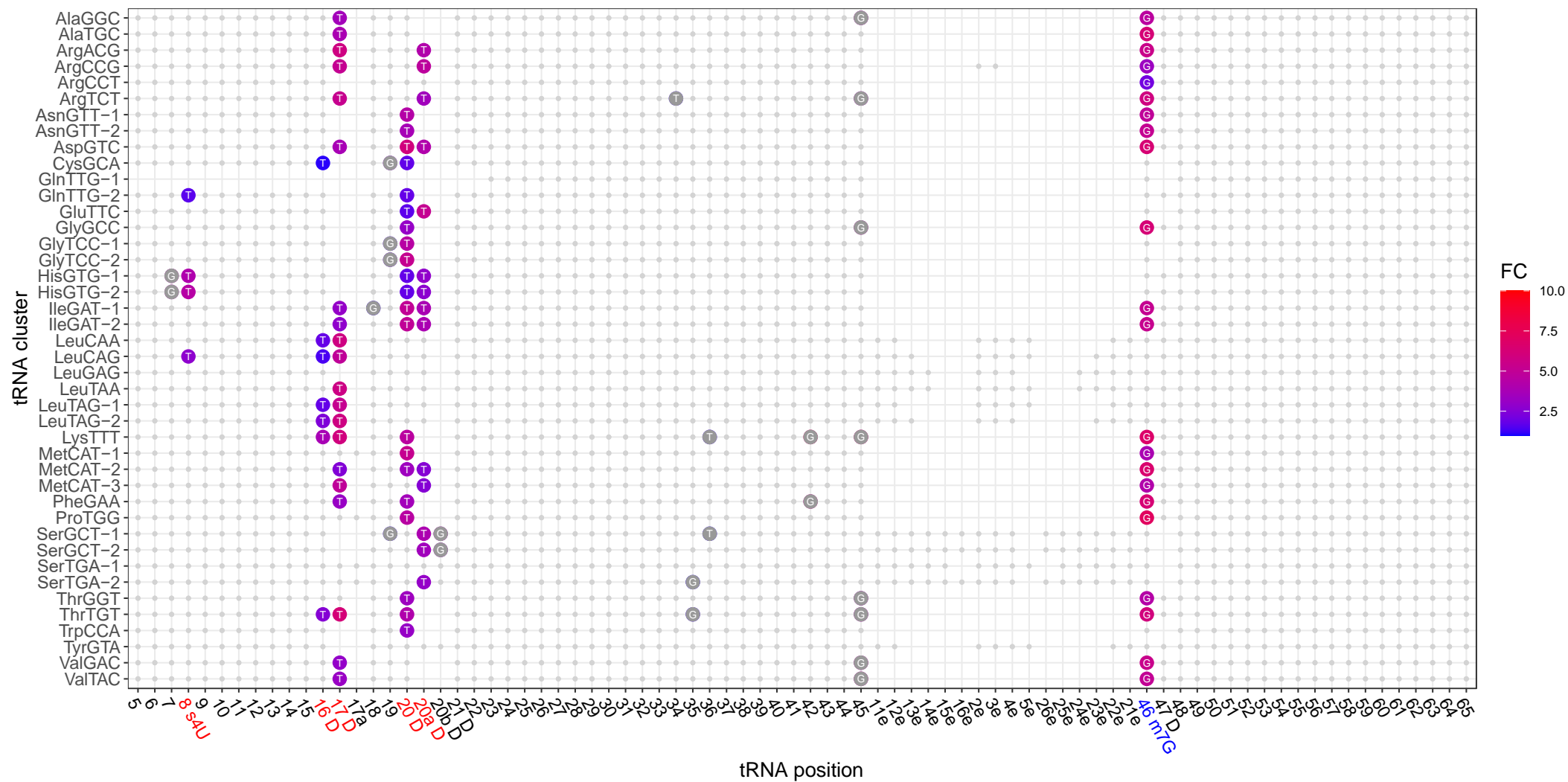


***E. sibiricum*, 30°C**

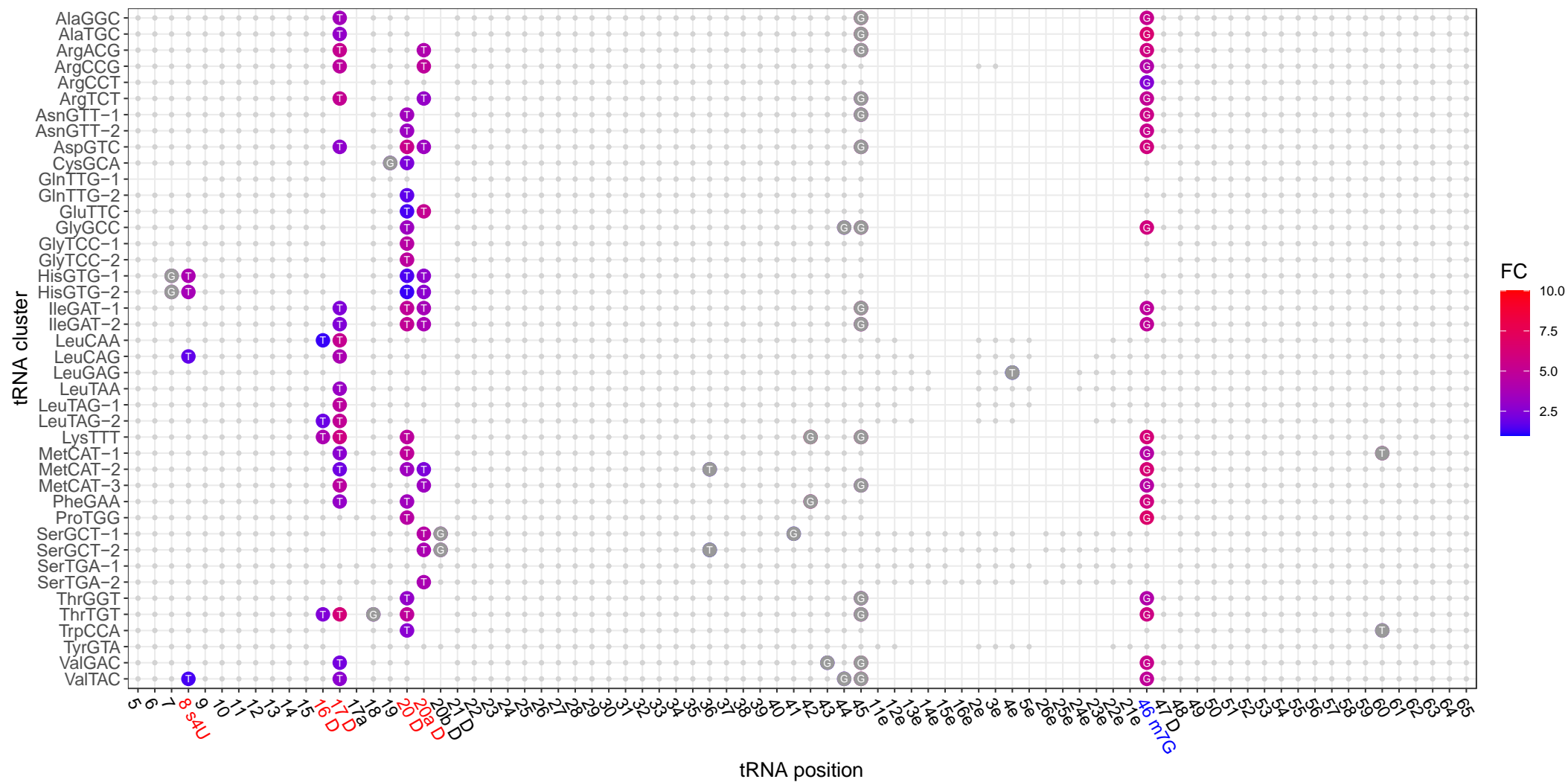


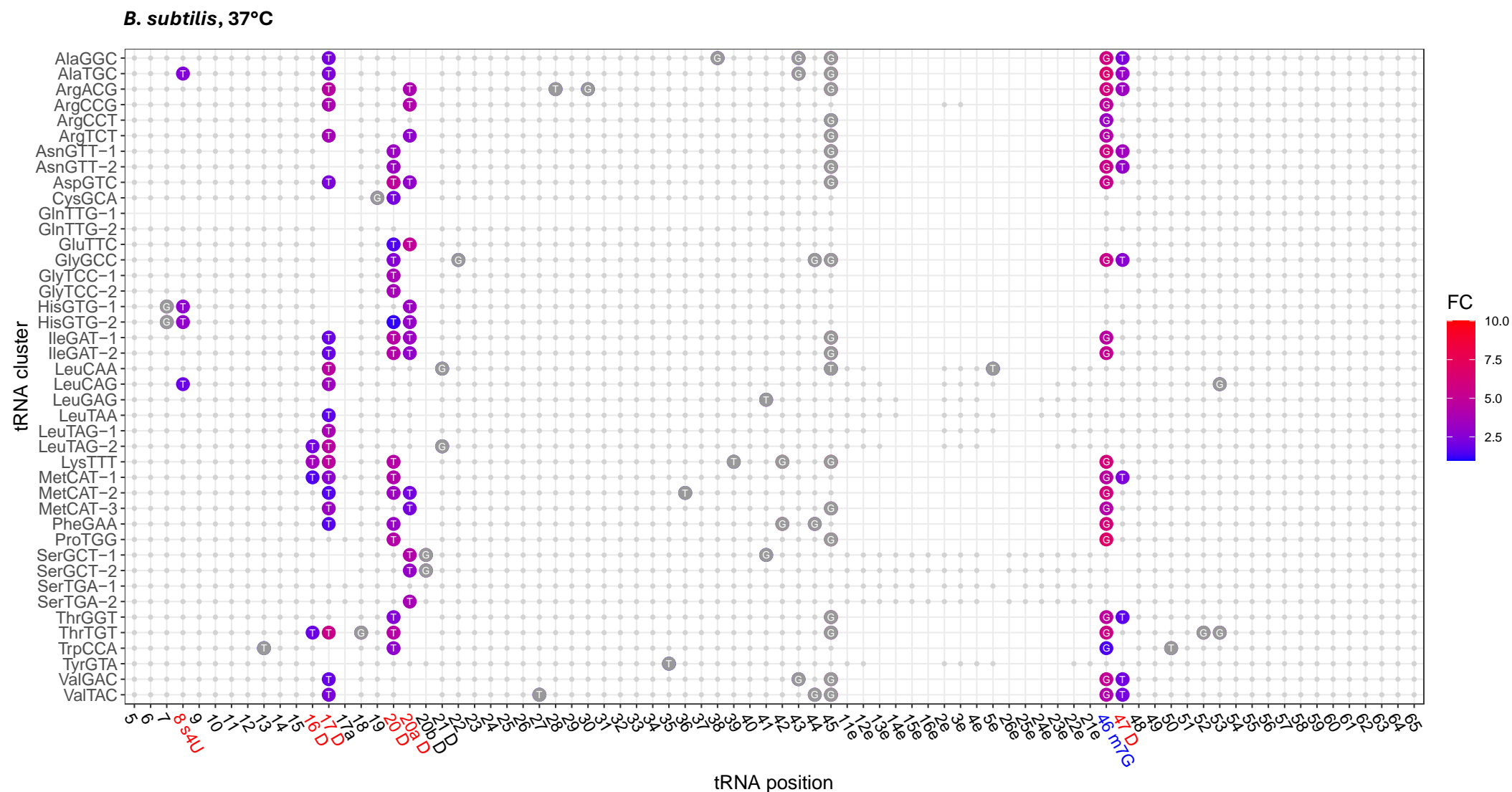
Suppl. Figure 4: Read termination sites from NaBH₄-treated RNA seq data of *E. sibiricum*. The figure illustrates the investigated RT sites for each tRNA cluster and tRNA position of *E. sibiricum* at each growth temperature studied. All tRNA positions exhibiting a significant (adj. P value < 0.01) and strong (FC ≥ 1, total number of RTs ≥ 20, and percentage of RTs ≥ 2) RT sites are color-coded from blue to red based on the logarithmic FC if the RT sites are classified as true positives. Type I false positive points are colored in gray. tRNA sites with no RT enrichment are represented as smaller gray dots. Enhanced RT sites were identified by comparing the RNA seq mapping profiles of NaBH₄-treated samples with those of untreated control samples.

***B. subtilis*, 20°C**



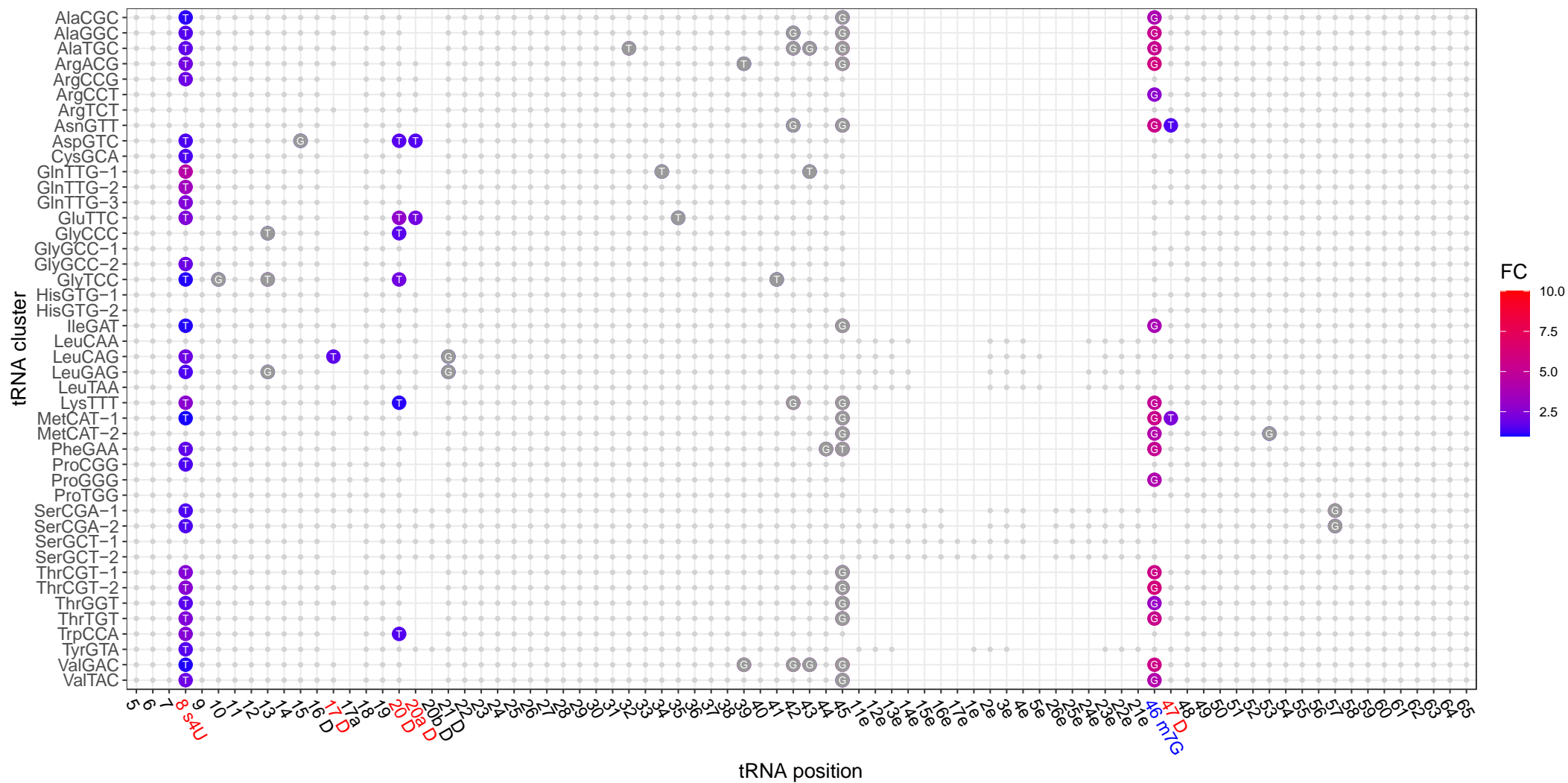
***B. subtilis*, 30°C**



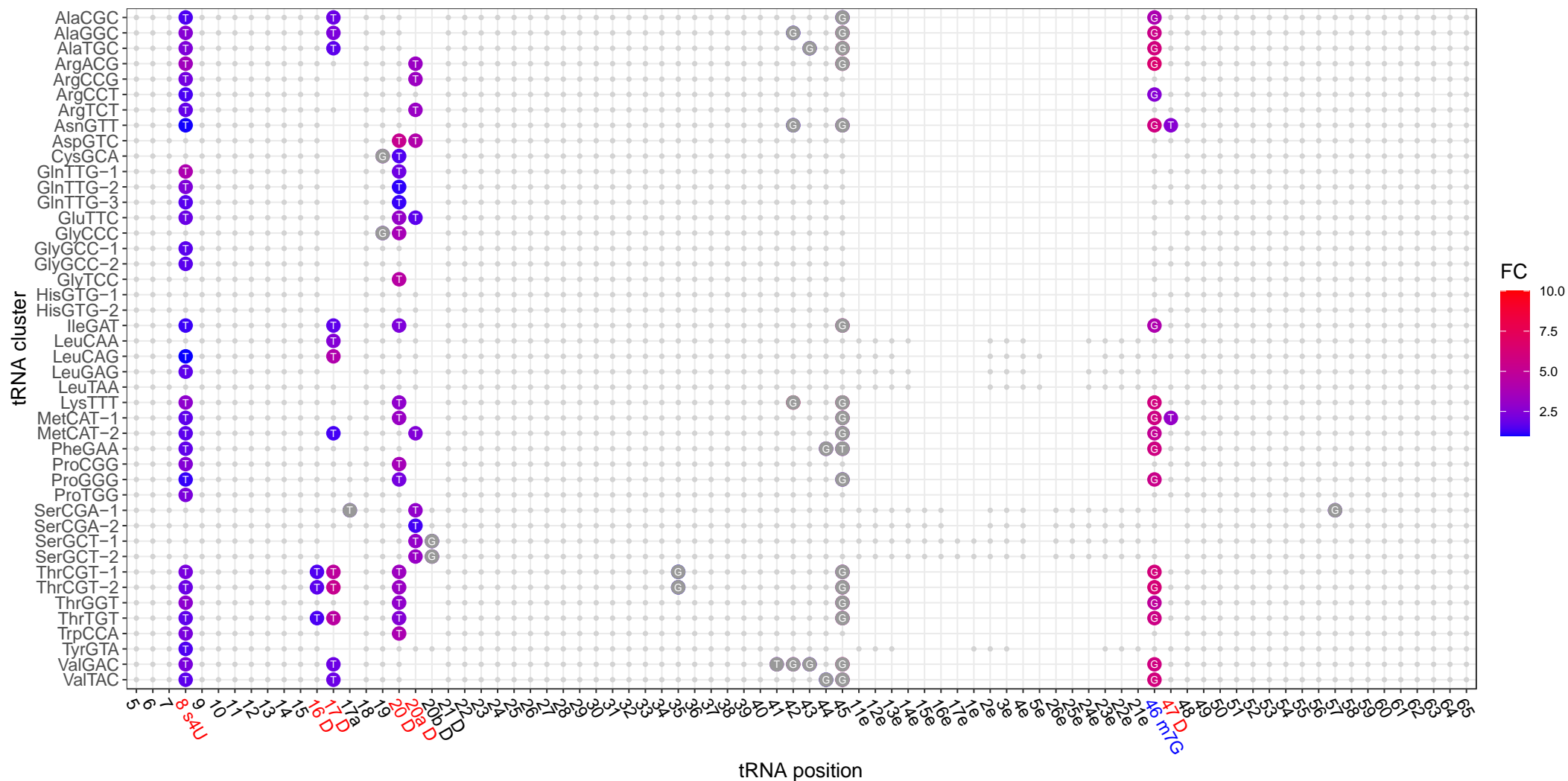


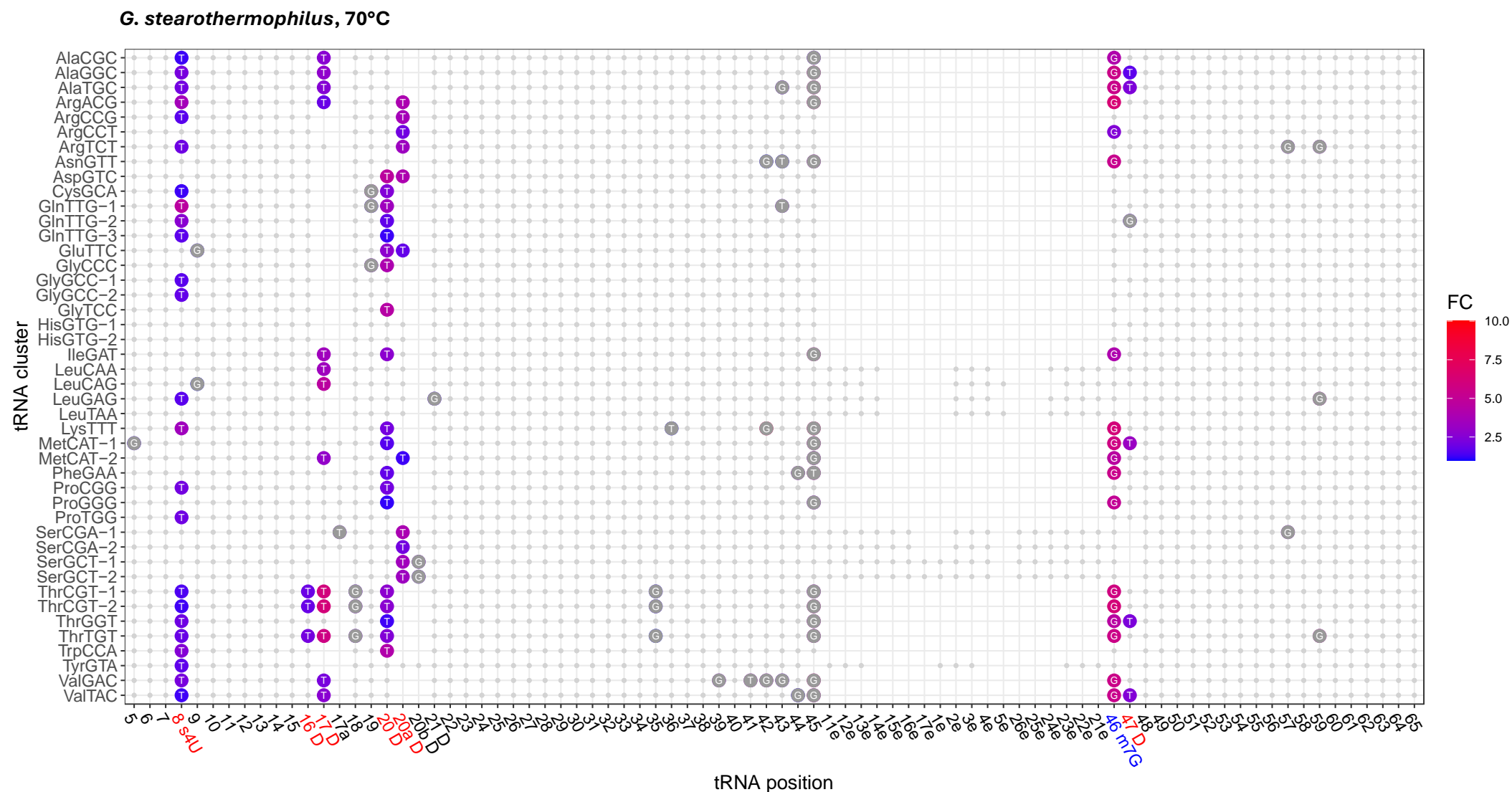
Suppl. Figure 5: Read termination sites from NaBH₄-treated RNA seq data of *B. subtilis*. The figure illustrates the investigated RT sites for each tRNA cluster and tRNA position of *B. subtilis* at each growth temperature studied. All tRNA positions exhibiting a significant (adj. P value < 0.01) and strong (FC ≥ 1, total number of RTs ≥ 20, and percentage of RTs ≥ 2) RT sites are color-coded from blue to red based on the logarithmic FC if the RT sites are classified as true positives. Type I false positive points are colored in gray. tRNA sites with no RT enrichment are represented as smaller gray dots. Enhanced RT sites were identified by comparing the RNA seq mapping profiles of NaBH₄-treated samples with those of untreated control samples.

***G. stearotherophilus*, 40°C**



***G. stearotherophilus*, 55°C**

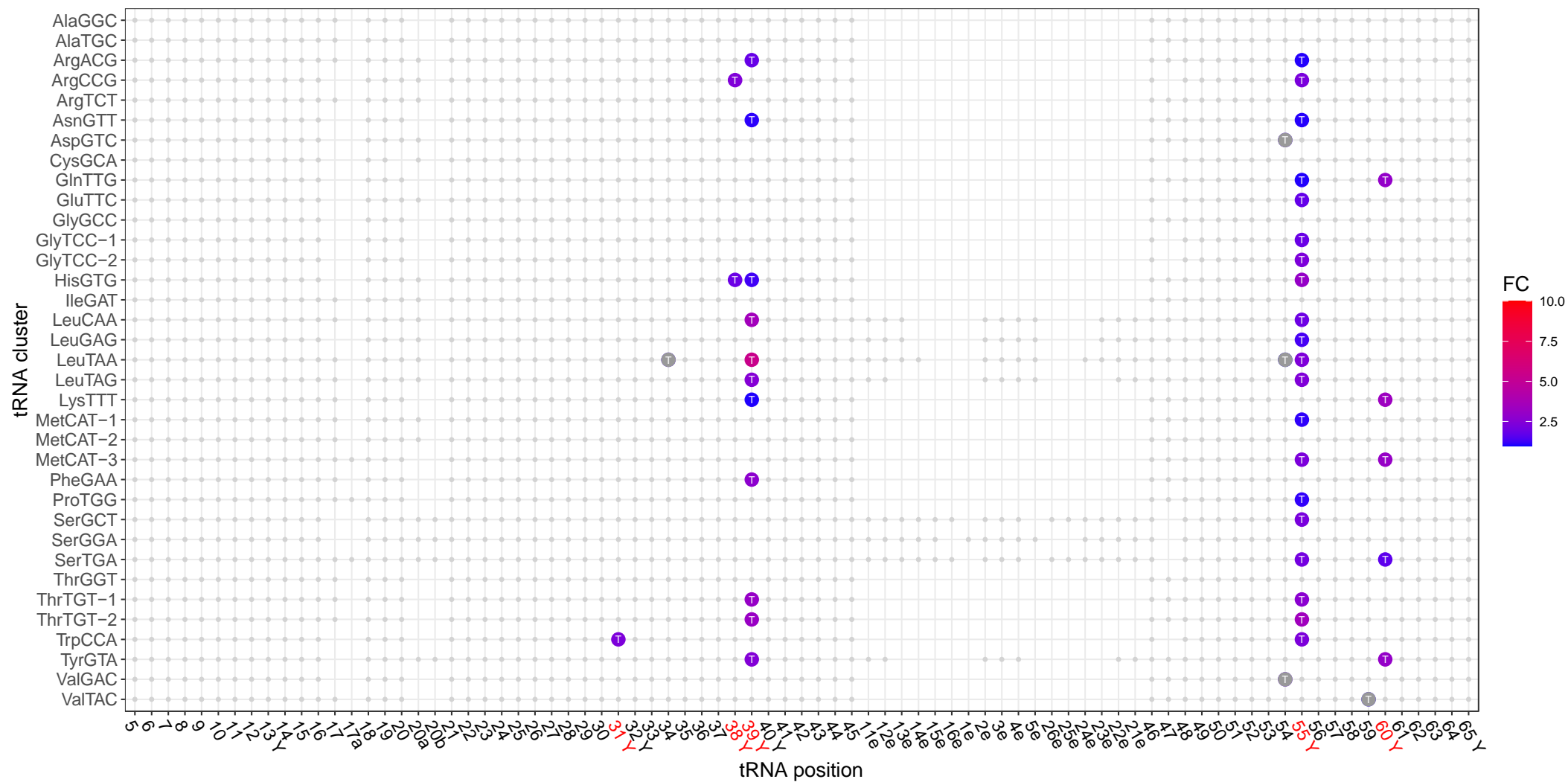


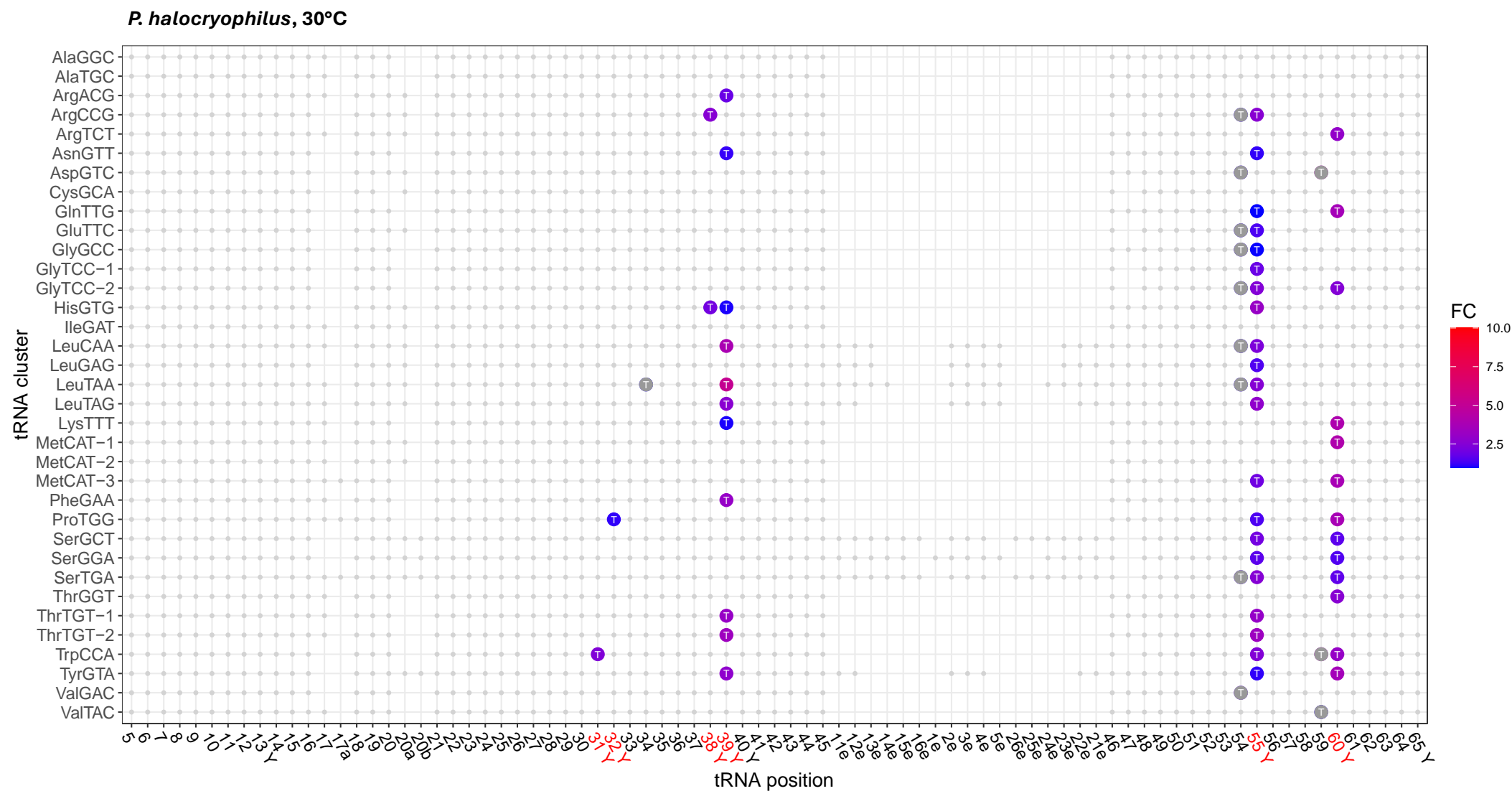


Suppl. Figure 6: Read termination sites from NaBH₄-treated RNA seq data of *G. stearothermophilus*. The figure illustrates the investigated RT sites for each tRNA cluster and tRNA position of *G. stearothermophilus* at each growth temperature studied. All tRNA positions exhibiting a significant (adj. P value < 0.01) and strong (FC ≥ 1, total number of RTs ≥ 20, and percentage of RTs ≥ 2) RT sites are color-coded from blue to red based on the logarithmic FC if the RT sites are classified as true positives. Type I false positive points are colored in gray. tRNA sites with no RT enrichment are represented as smaller gray dots. Enhanced RT sites were identified by comparing the RNA seq mapping profiles of NaBH₄-treated samples with those of untreated control samples.



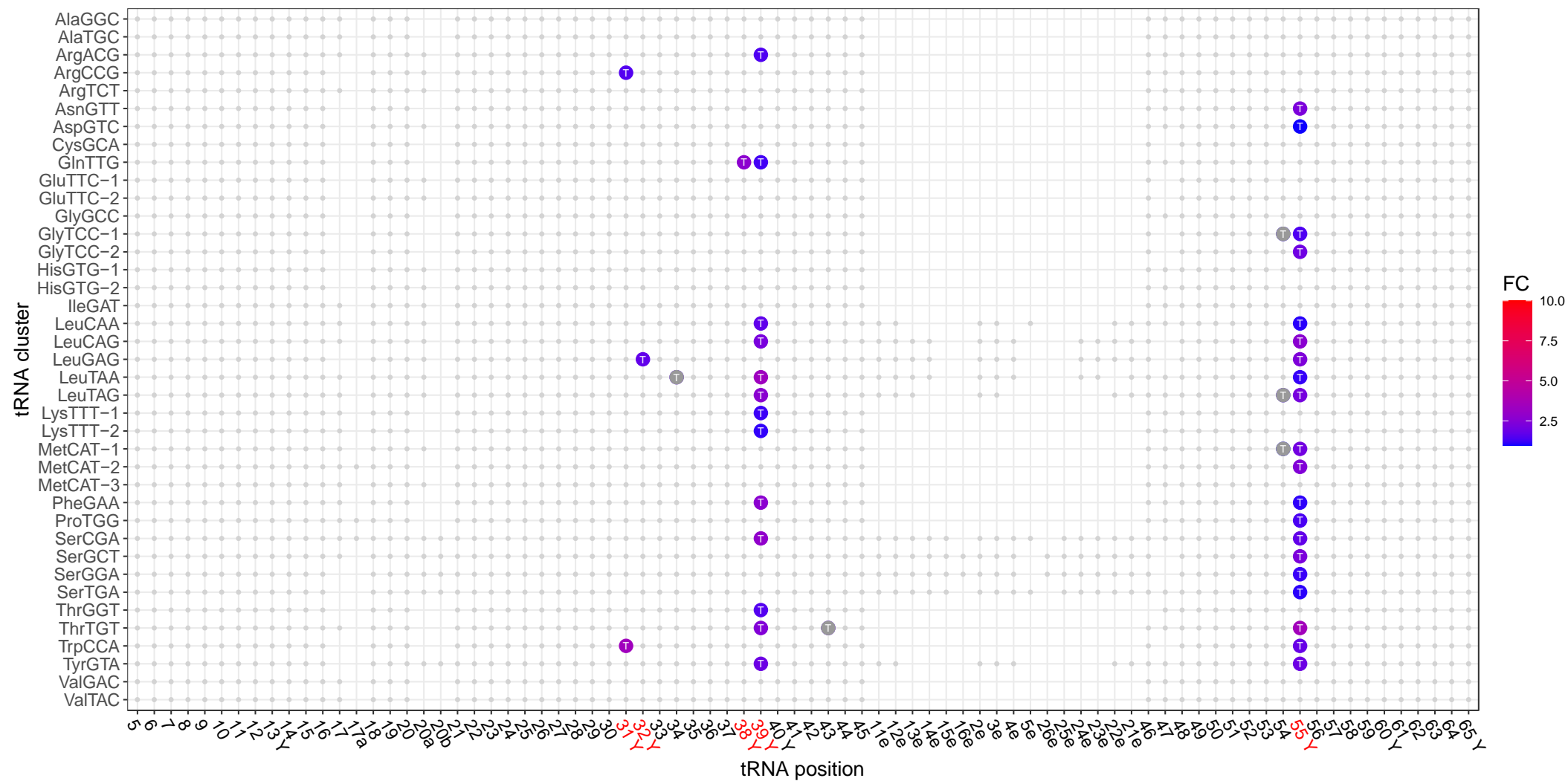
***P. halocryophilus*, 20°C**



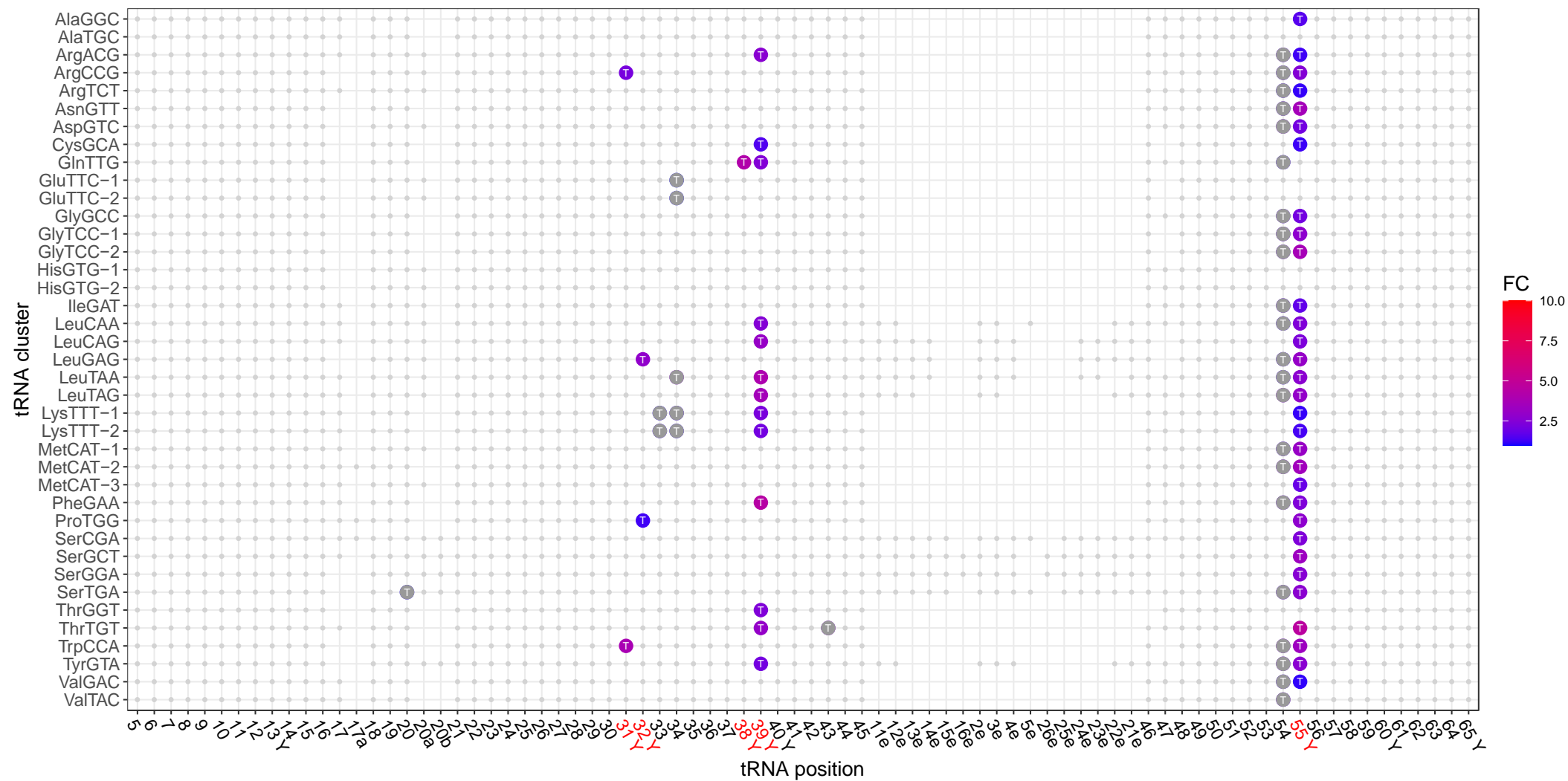


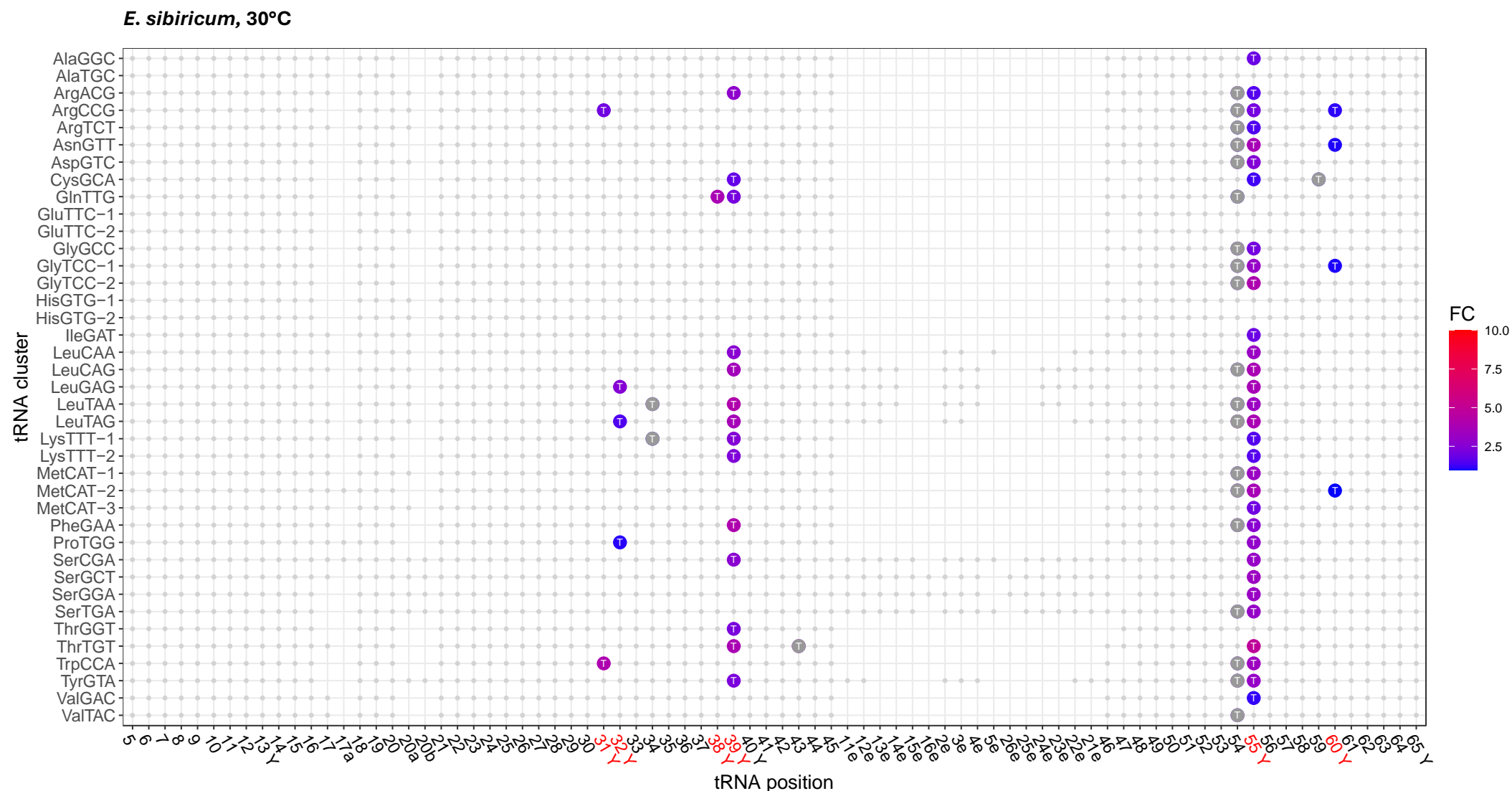
Suppl. Figure 7: Read termination sites from CMCT-treated RNA seq data of *P. halocryophilus*. The figure illustrates the investigated RT sites for each tRNA cluster and tRNA position of *P. halocryophilus* at each growth temperature studied. All tRNA positions exhibiting a significant (adj. P value < 0.01) and strong (FC ≥ 1, total number of RTs ≥ 20, and percentage of RTs ≥ 3) RT sites are color-coded from blue to red based on the logarithmic FC if the RT sites are classified as true positives. Type I false positive points are colored in gray. tRNA sites with no RT enrichment are represented as smaller gray dots. Enhanced RT sites were identified by comparing the RNA seq mapping profiles of 1-cyclohexyl-(2-morpholinoethyl)carbodiimide metho-p-toluene sulfonate (CMCT)-treated samples with those of untreated control samples.

***E. sibiricum*, 10°C**



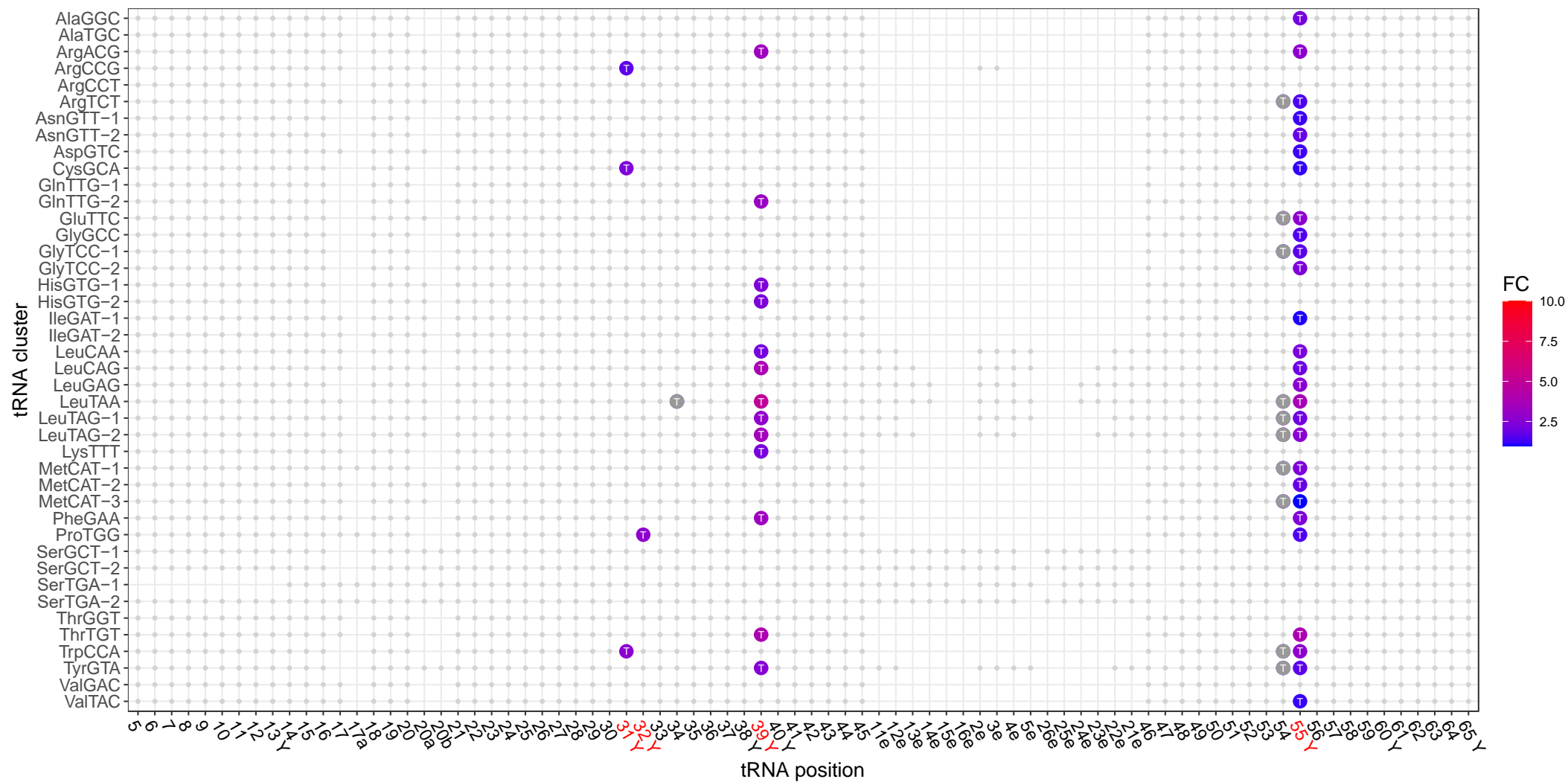
***E. sibiricum*, 20°C**



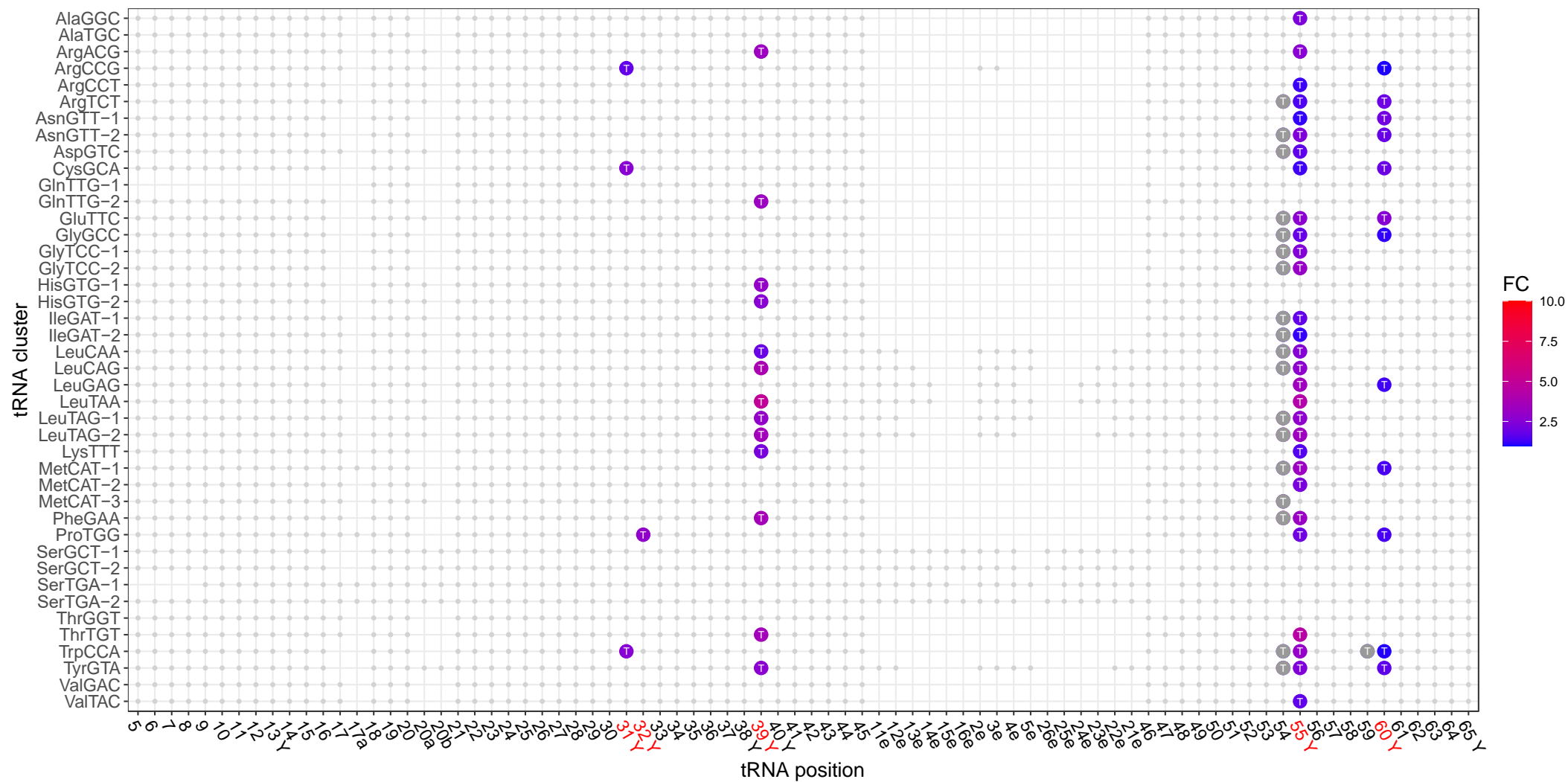


Suppl. Figure 8: Read termination sites from CMCT-treated RNA seq data of *E. sibiricum*. The figure illustrates the investigated RT sites for each tRNA cluster and tRNA position of *E. sibiricum* at each growth temperature studied. All tRNA positions exhibiting a significant (adj. P value < 0.01) and strong (FC ≥ 1, total number of RTs ≥ 20, and percentage of RTs ≥ 3) RT sites are color-coded from blue to red based on the logarithmic FC if the RT sites are classified as true positives. Type I false positive points are colored in gray. tRNA sites with no RT enrichment are represented as smaller gray dots. Enhanced RT sites were identified by comparing the RNA seq mapping profiles of CMCT-treated samples with those of untreated control samples.

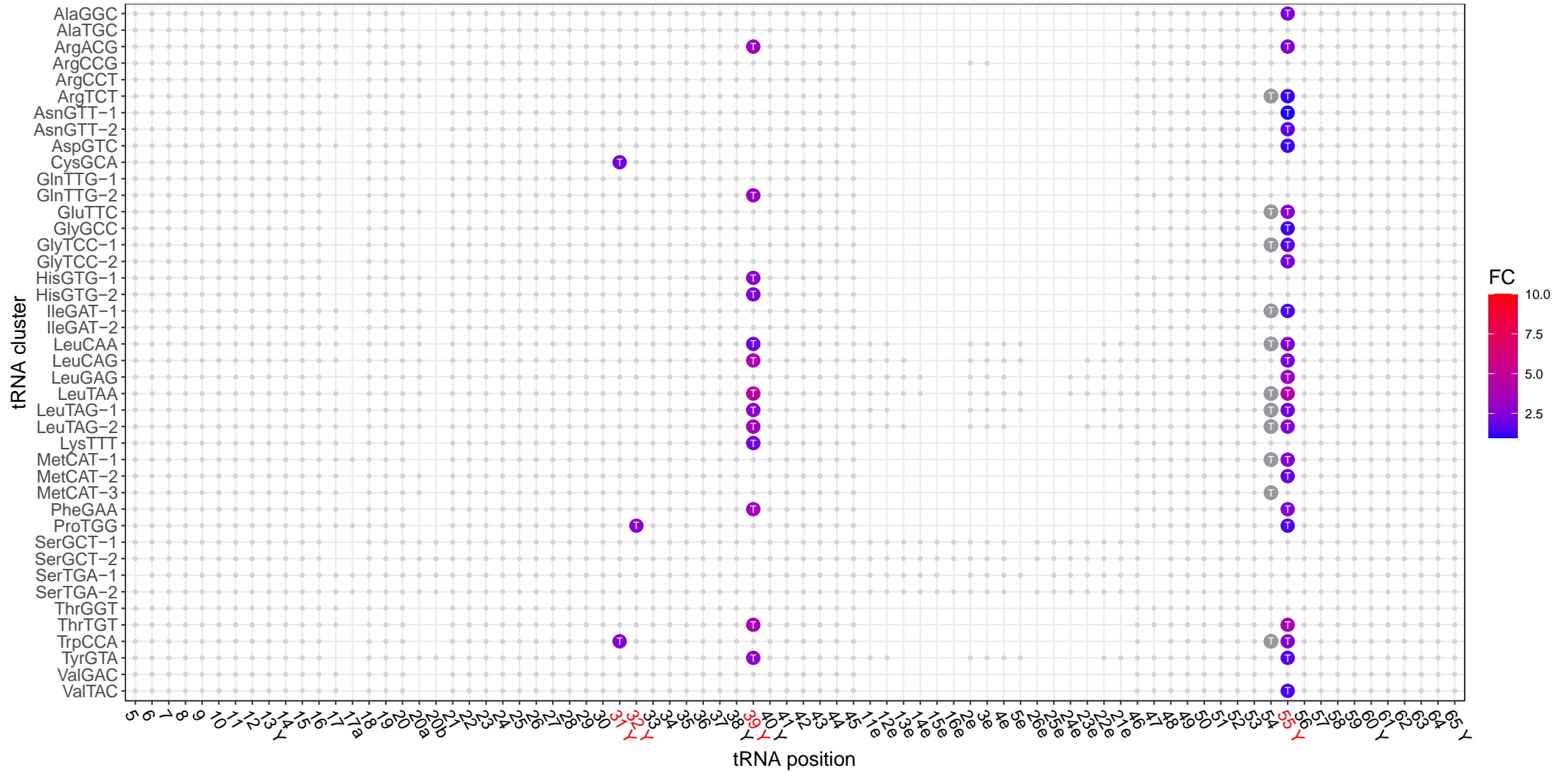
***B. subtilis*, 20°C**



***B. subtilis*, 30°C**

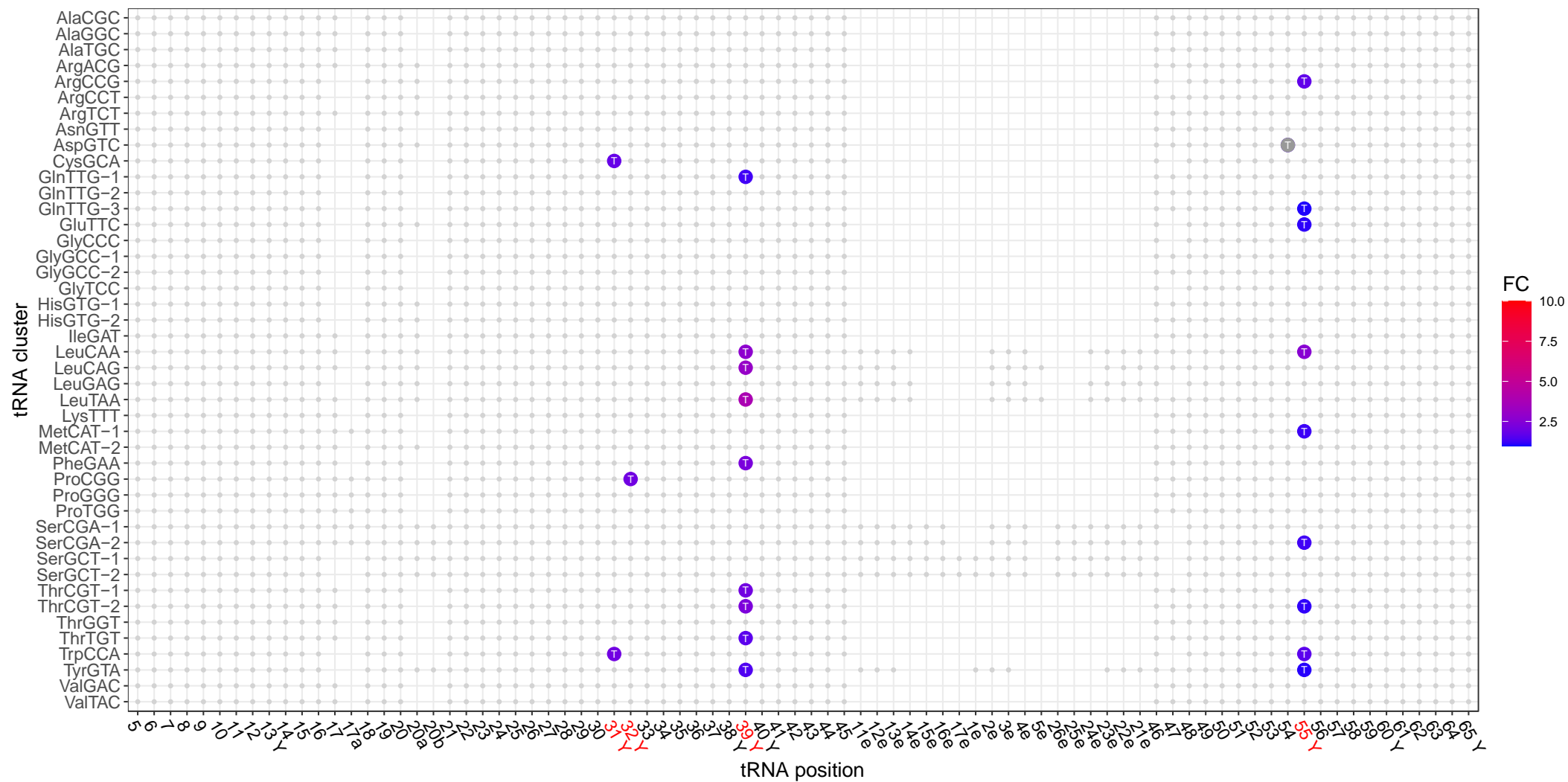


***B. subtilis*, 37°C**

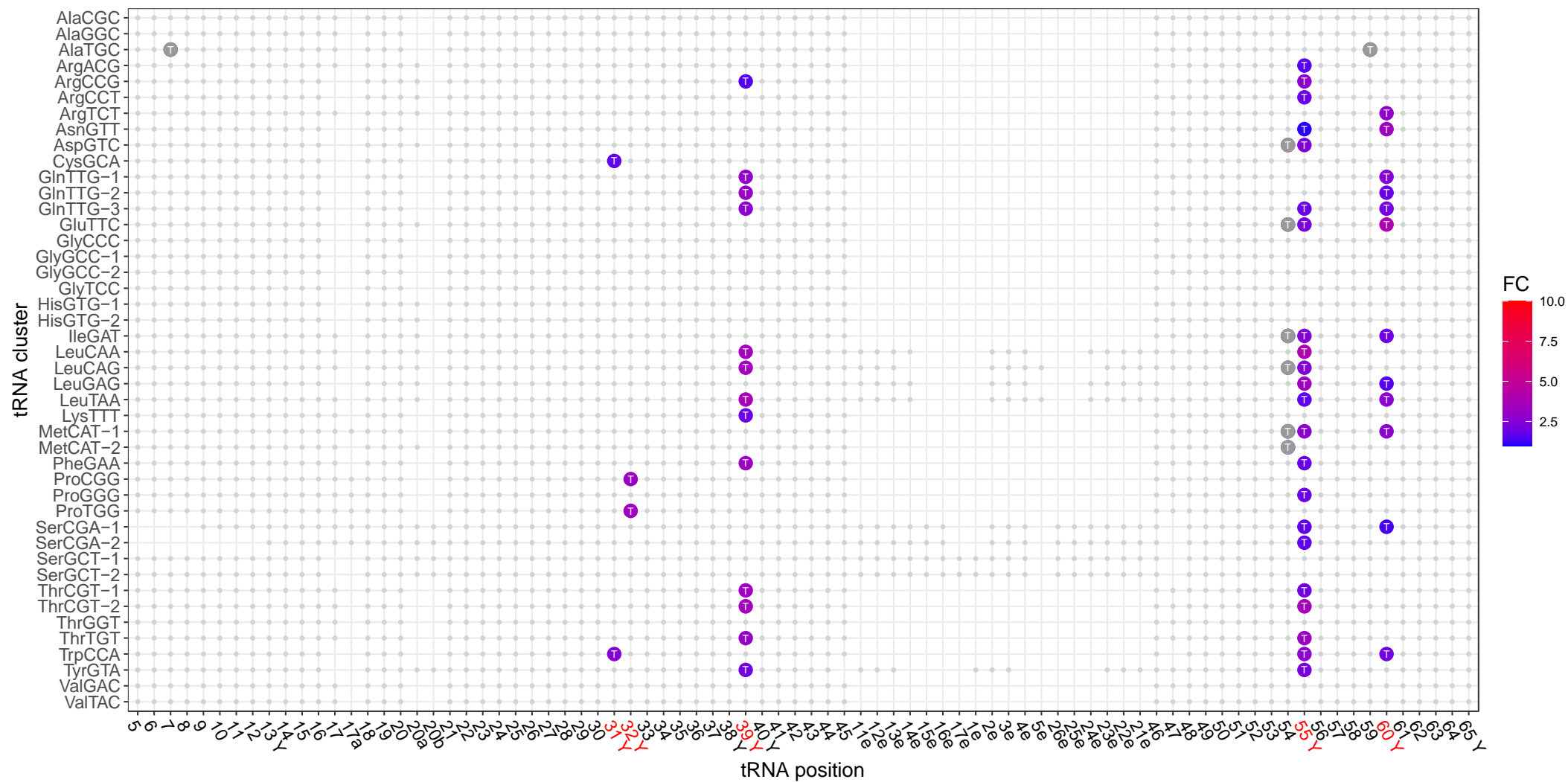


Suppl. Figure 9: Read termination sites from CMCT-treated RNA seq data of *B. subtilis*. The figure illustrates the investigated RT sites for each tRNA cluster and tRNA position of *B. subtilis* at each growth temperature studied. All tRNA positions exhibiting a significant (adj. P value < 0.01) and strong (FC ≥ 1, total number of RTs ≥ 20, and percentage of RTs ≥ 3) RT sites are color-coded from blue to red based on the logarithmic FC if the RT sites are classified as true positives. Type I false positive points are colored in gray. tRNA sites with no RT enrichment are represented as smaller gray dots. Enhanced RT sites were identified by comparing the RNA seq mapping profiles of CMCT-treated samples with those of untreated control samples.

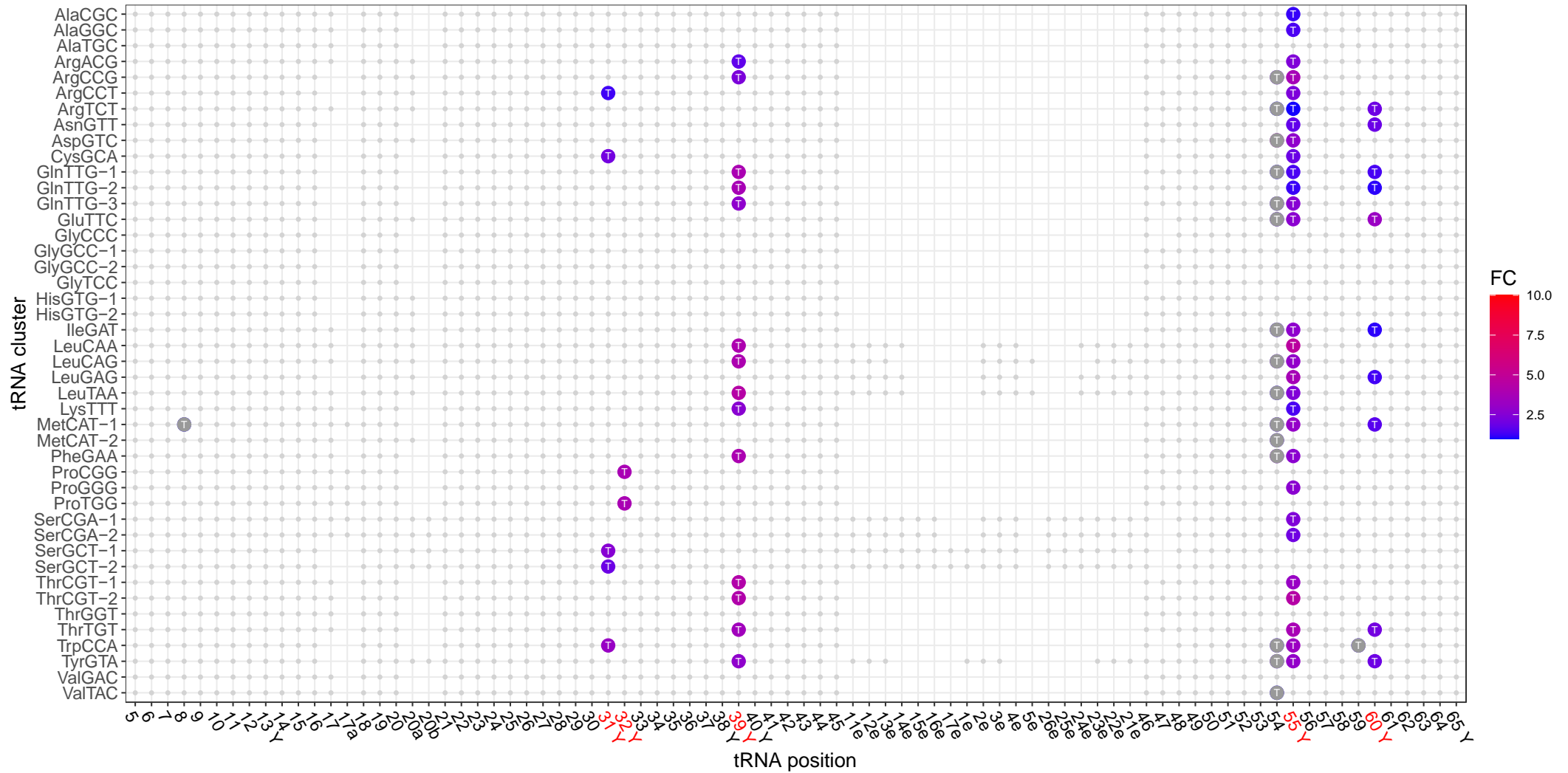
***G. stearothermophilus*, 40°C**



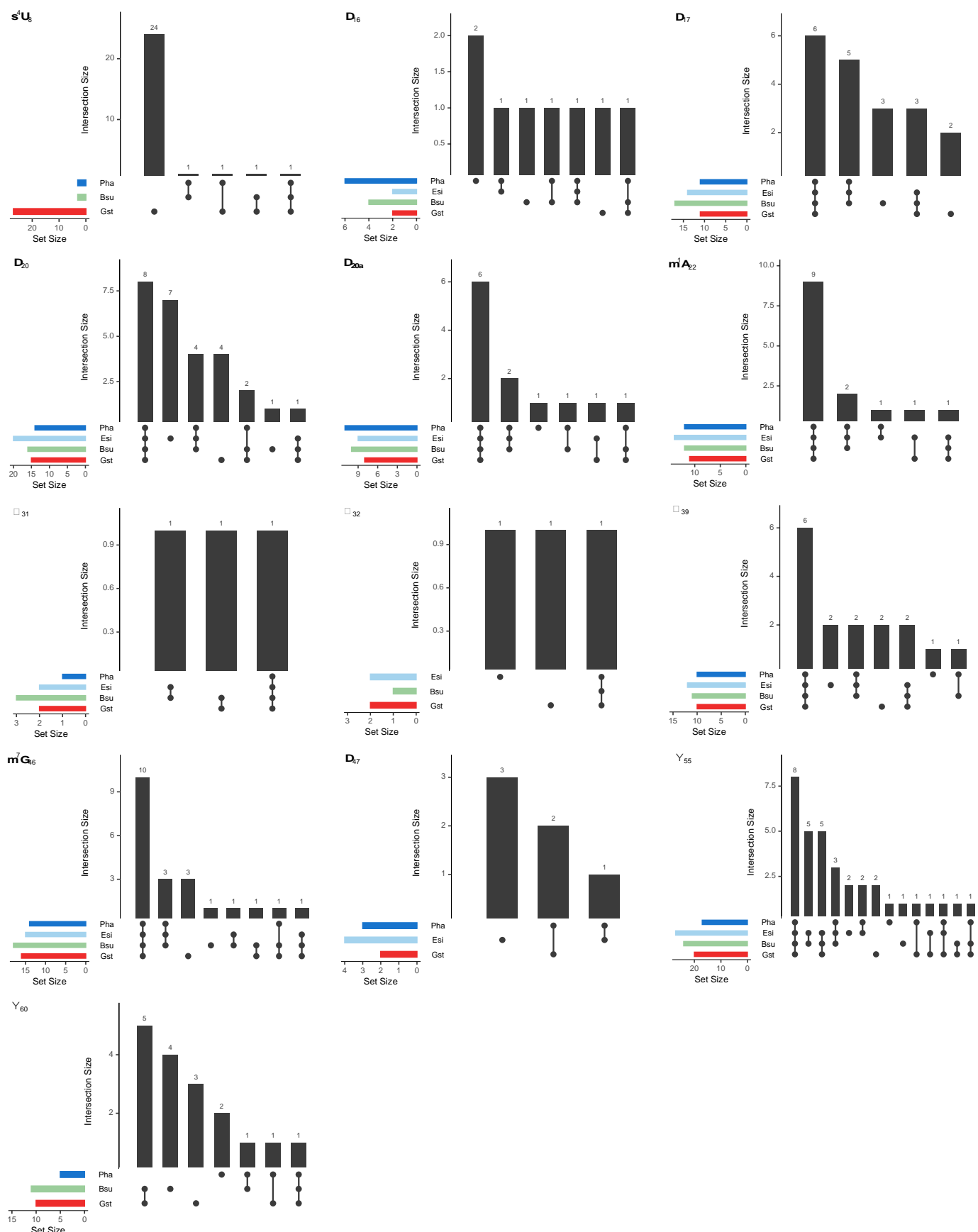
***G. stearothermophilus*, 55°C**



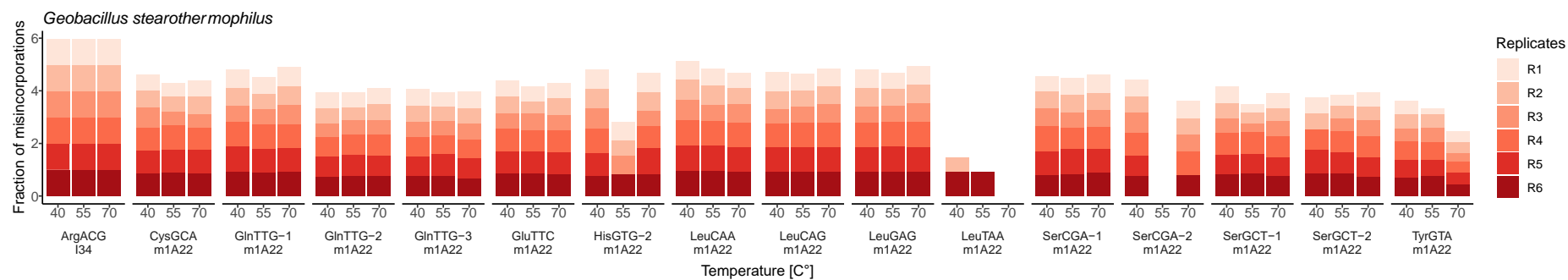
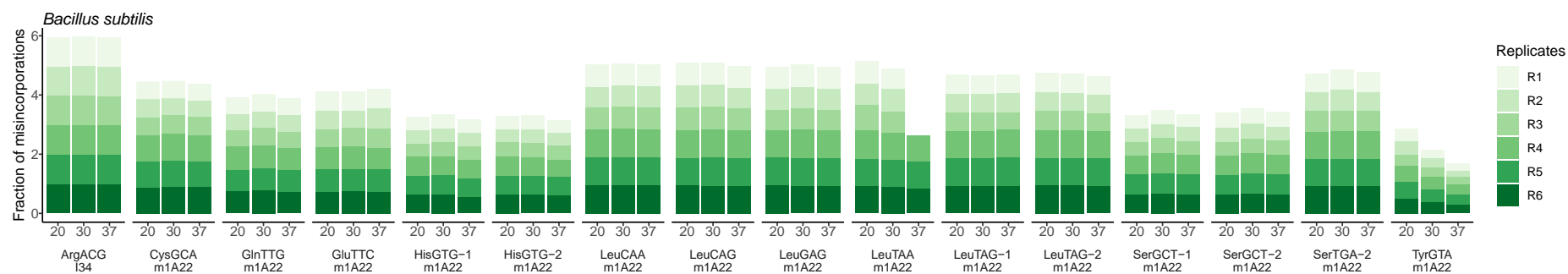
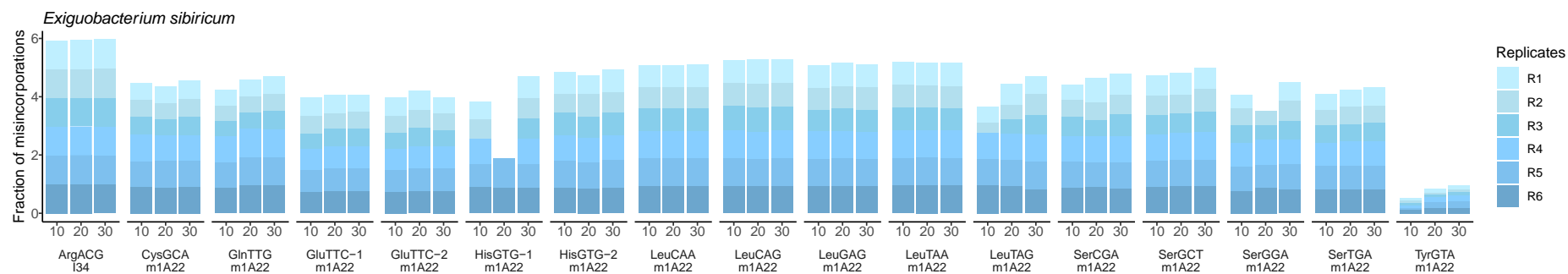
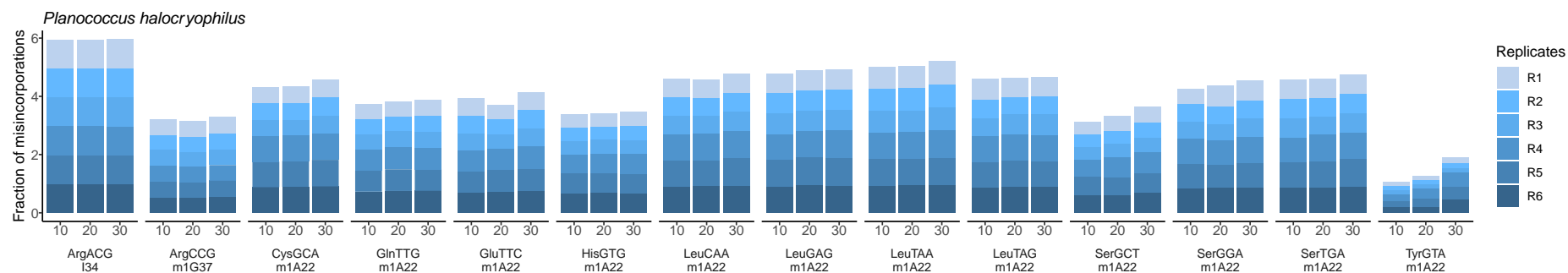
***G. stearothermophilus*, 70°C**



Suppl. Figure 10: Read termination sites from CMCT-treated RNA seq data of *G. stearothermophilus*. The figure illustrates the investigated RT sites for each tRNA cluster and tRNA position of *G. stearothermophilus* at each growth temperature studied. All tRNA positions exhibiting a significant (adj. P value < 0.01) and strong (FC ≥ 1, total number of RTs ≥ 20, and percentage of RTs ≥ 3) RT sites are color-coded from blue to red based on the logarithmic FC if the RT sites are classified as true positives. Type I false positive points are colored in gray. tRNA sites with no RT enrichment are represented as smaller gray dots. Enhanced RT sites were identified by comparing the RNA seq mapping profiles of CMCT-treated samples with those of untreated control samples.



Suppl. Figure 11: Overlap in the numbers of modified tRNA families across different bacteria. Upset plots depict the intersection of modified tRNA families categorized by their encoded amino acids and their respective anticodons (unique counts). The counts are derived from RNA sequencing data obtained at the optimal growth temperatures of the cultured bacteria, which are 20°C for *P. halocryophilus* and *E. sibiricum*, 30°C for *B. subtilis*, and 55°C for *G. stearothermophilus*



Suppl. Figure 12: Fraction of base mismatches for m¹A, I and m¹G tRNA modifications. The fraction of misincorporations [nucleotide mismatches / original nucleotide] in the mapping profile at positions 22, 34, and 37 are shown for each affected tRNA, as well as the investigated bacteria and temperatures. The proportion of misincorporations is given for each biological replicate [R1-R6] and these were only considered if more than 20 reads were available. Inosine (I)34 and 1-methyladenosine (m¹A)22 were identified in each bacterium, while 1-methylguanosine (m¹G)37 was only found at tRNA^{Arg}_{CCG} of *P. halocryophilus*.